NUMERICAL ANALYSIS OF GROUND-WATER FLOW AND SALINITY IN THE EWA AREA, OAHU, HAWAII

By Delwyn S. Oki, William R. Souza, Edward L. Bolke, and Glenn R. Bauer

---

U.S. GEOLOGICAL SURVEY

Open-File Report 96-442

Prepared in cooperation with the

STATE OF HAWAII
COMMISSION ON WATER RESOURCE MANAGEMENT

Honolulu, Hawaii
1996

U.S. DEPARTMENT OF THE INTERIOR
BRUCE BABBITT, Secretary

U.S. GEOLOGICAL SURVEY
Gordon P. Eaton, Director

For sale by the U.S. Geological Survey
Branch of Information Services
Box 25286
Denver CO 80225-0286

For additional information write to:
District Chief
U.S. Geological Survey
677 Ala Moana Blvd., Suite 415
Honolulu, HI 96813

CONTENTS

FIGURES

TABLES

Conversion Factors

Multiply	By	To obtain
foot (ft)	0.3048	meter
mile (mi)	1.609	kilometer
inch (in.)	25.4	millimeter
foot per day (ft/d)	0.3048	meter per day
foot per mile (ft/mi)	0.1894	meter per kilometer
million gallons per day (Mgal/d)	0.04381	cubic meter per second

Numerical Analysis of Ground-Water Flow and Salinity in the Ewa Area, Oahu, Hawaii

By Delwyn S. Oki, William R. Souza, Edward L. Bolke, and Glenn R. Bauer

Abstract

The coastal plain in the Ewa area of southwestern Oahu, Hawaii, is part of a larger, nearly continuous sedimentary coastal plain along Oahu's southern coast. The coastal sediments are collectively known as caprock because they impede the free discharge of ground water from the underlying volcanic aquifers. The caprock is a layered sedimentary system consisting of interbedded marine and terrestrial sediments of both high and low permeability. Before sugarcane cultivation ended in late 1994, shallow ground water from the upper limestone unit, which is about 60 to 200 feet thick, was used primarily for irrigation of sugarcane.

A cross-sectional ground-water flow and transport model was used to evaluate the hydrogeologic controls on the regional flow system in the Ewa area. Controls considered were: (1) overall caprock hydraulic conductivity, (2) stratigraphic variations of hydraulic conductivity in the caprock, and (3) recharge. In addition, the effects of a marina excavation were evaluated.

Within the caprock, variations in hydraulic conductivity, caused by caprock stratigraphy or discontinuities of the stratigraphic units, are a major control on the direction of ground-water flow and the distribution of water levels and salinity. Model results also show that a reduction of recharge will result in increased salinity throughout the caprock with the greatest change in the upper limestone layer. In addition, the model indicates that excavation of an ocean marina will lower water levels in the upper limestone layer.

Results of cross-sectional modeling confirm the general ground-water flow pattern that would be expected in the layered sedimentary system in the Ewa caprock. Ground-water flow is: (1) predominantly upward in the low-permeability sedimentary units, and (2) predominantly horizontal in the high-permeability sedimentary units.

INTRODUCTION

The coastal plain in the Ewa area of Oahu is a broad, flat plain composed of interbedded marine and terrestrial sediments, extending from the west side of Pearl Harbor to Kahe Point (fig. 1). The coastal plain in the Ewa area is part of a larger nearly continuous sedimentary plain that forms the south shore of Oahu from Kahe Point to the east side of Honolulu. The coastal sediments are locally referred to as caprock because they impede the free discharge of ground water from the underlying volcanic aquifers. The coastal plain near Ewa comprises an area of about 28 mi^2 (Lau and others, 1986), and extends inland from the shoreline 2.5 mi in the western part near Barbers Point to almost 5 mi in the eastern part near Pearl Harbor (George A.L. Yuen and Associates, Inc., 1989) (fig. 2).

For most of the year the Ewa area is hot and dry. The 30-year average maximum temperature at Ewa Plantation Mill (State key no. 741) is 83.9°F, while the average minimum is 65.9°F. (Owenby and Ezell, 1992). Average maximum and minimum temperatures at the Honolulu Observatory (State key no. 702.2) in Ewa Beach are about a degree warmer than at Ewa Plantation Mill. Average maximum summer temperatures over the Ewa area range from 80 to 85°F. The 30-year average annual rainfall is 21.5 in/yr and 22.8 in/yr at

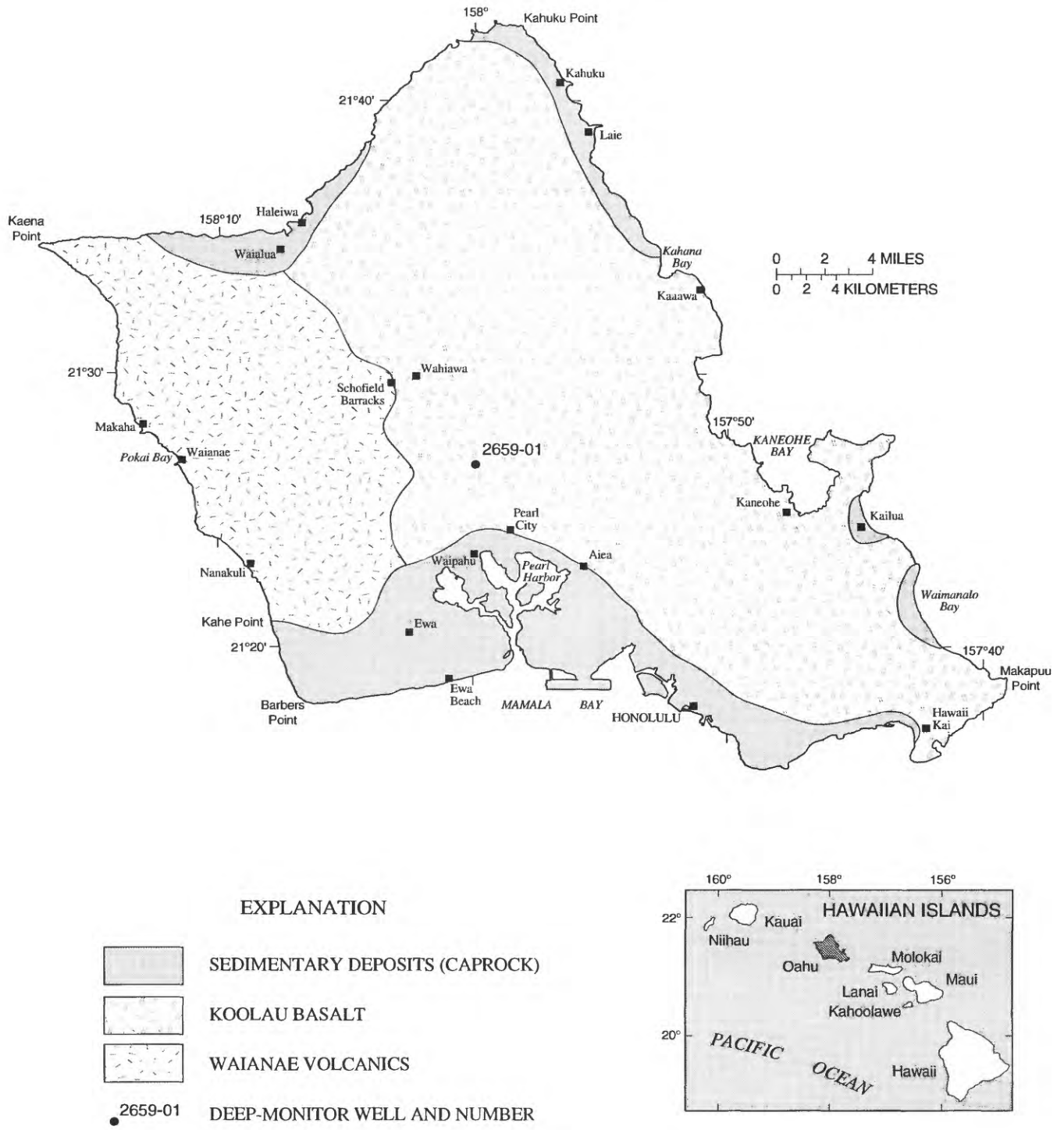

Figure 1. Generalized geology of Oahu, Hawaii (modified from Stearns, 1946).

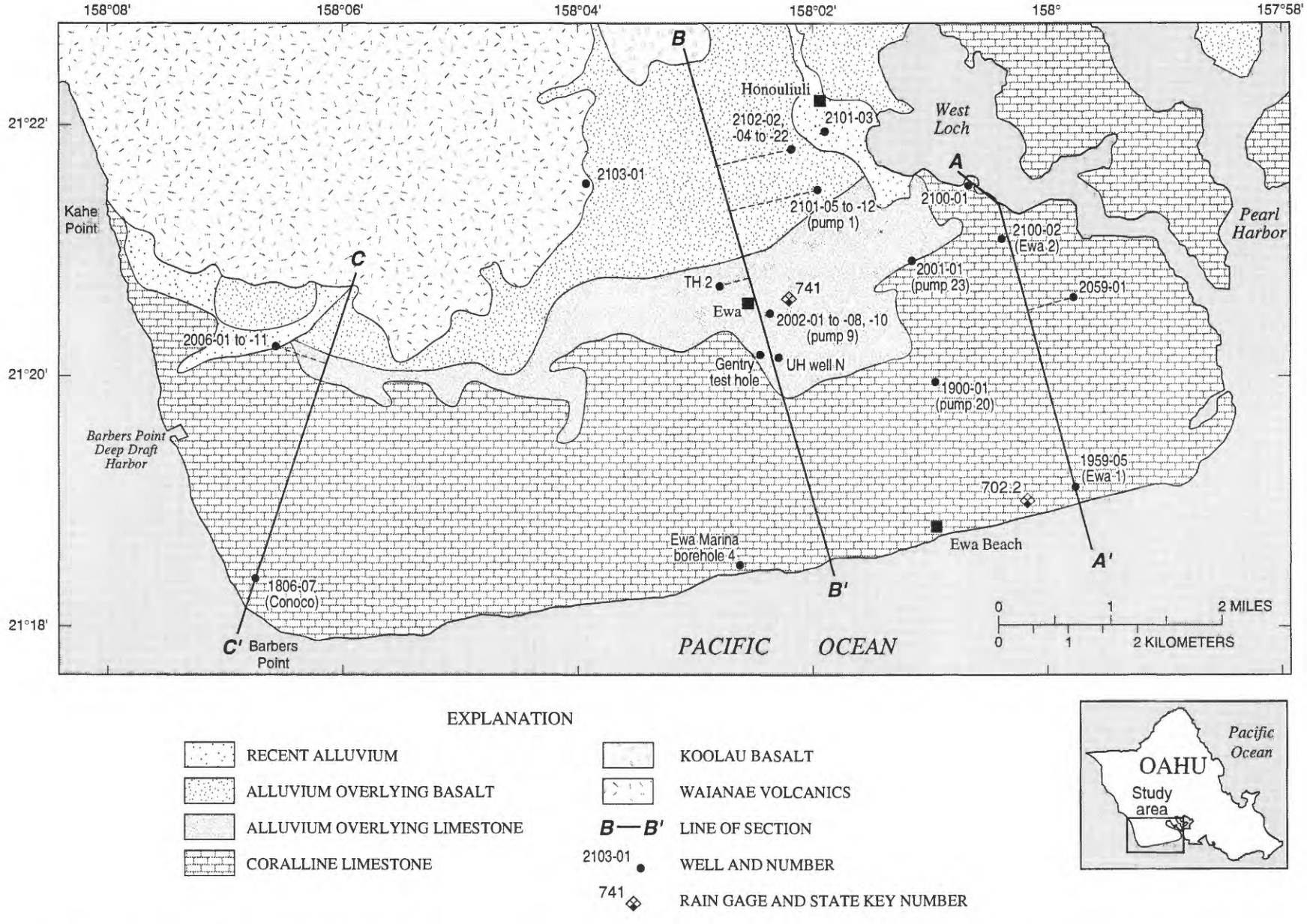

Figure 2. Geology of the coastal plain in the Ewa area, Oahu, Hawaii (modified from George A.L. Yuen and Associates, Inc., 1989).

Honolulu Observatory and at Ewa Plantation Mill, respectively (Owenby and Ezell, 1992). Most of the precipitation is from a few intense island-wide winter storms from November through April.

In the Ewa area, ground water is pumped from the Waianae and Koolau volcanic aquifers as well as from permeable units in the caprock overlying the volcanic rocks. Historically, both fresh and brackish ground water have been used heavily for sugarcane cultivation, landscaping, and golf course maintenance. Until the early 1980's, sugarcane irrigation was the largest single use of ground water in the Ewa area. However, beginning in the early 1980's, the use of ground water for sugarcane cultivation began declining. During this same period, ground-water demands for other uses, including urban development, industry, and diversified agriculture, were increasing. By November 1994, sugarcane operations in the Ewa area ceased. The end of sugarcane cultivation resulted in a large reduction of return-irrigation water, thus eliminating a large source of recharge to the shallow ground water in the caprock. Prudent management of the ground-water resources of the Ewa area requires an understanding of the ground-water flow system in the volcanic aquifers and in the caprock.

The objective of this study was to develop a refined conceptual model of the ground-water flow system in the Ewa caprock by identifying the major hydrogeologic controls on the regional movement of ground water and the salinity distribution within the caprock. This report on the Ewa area includes (1) a description of the hydrogeologic setting, (2) a description of a preliminary, two-dimensional, cross-sectional, ground-water flow and transport model, (3) results of selected model scenarios designed to identify the major hydrogeologic controls on ground-water flow and salinity, (4) a discussion of possible effects of the end of sugarcane cultivation and excavation of an ocean marina, and (5) a description of a refined conceptual model of the ground-water flow system.

HISTORY OF GROUND-WATER DEVELOPMENT

Pumpage.--Before sugarcane cultivation, the Ewa area did not support agriculture of any significance because of limited water resources. In 1879 the first artesian well in Hawaii was drilled on land owned by James Campbell near the town of Honouliuli (fig. 2). This well completely penetrated sedimentary rocks of the caprock and entered into the underlying volcanic aquifer where the water level rose to an elevation of 32 ft above mean sea level (Thrum, 1889; Mink, 1980). Before this well was drilled, water development consisted of shallow dug wells, rain catchment, low-level springs, and streams. By the end of 1884, there were 19 wells drilled in the Ewa area (Cox, 1981). In 1890, ten additional wells were drilled specifically for sugarcane irrigation in Ewa, near the village of Honouliuli. These wells were located at elevations too high for artesian flow so steam pumps were required (Cox, 1981). Once the Ewa Plantation began operation in 1890, 650 acres of sugarcane were planted near Honouliuli on the alluvial portion (fig. 2) of the coastal plain in the Ewa area (Stearns and Vaksvik, 1935; George A.L. Yuen and Associates, Inc., 1989). In 1930, Ewa Plantation pumped about 72.5 Mgal/d from the volcanic aquifers in the Ewa area (Stearns and Vaksvik, 1935, p. 311).

Starting about 1930, Ewa Plantation began drilling shallow wells in the sedimentary deposits of the caprock to irrigate more sugarcane acreage. These wells were drilled seaward of the wells at Honouliuli. Pumpage of ground water from the caprock wells averaged about 12 Mgal/d until 1964. In 1964 several new caprock wells were drilled and pumpage subsequently increased to 20 Mgal/d. Ewa Plantation shut down in 1970 and was consolidated under Oahu Sugar Company. In 1981, pumpage from caprock wells increased to 31 Mgal/d. Furrow irrigation of sugarcane was used until the early 1980's when this method was completely replaced by drip irrigation. Following the conversion from furrow to drip irrigation, average pumpage in the 1980's decreased to between 15 and 20 Mgal/d (fig. 3). Sugarcane cultivation in the Ewa area ceased in 1994, and pumpage from the caprock in the Ewa area was thus reduced to less than 5 Mgal/d.

Beginning in the late 1970's, new housing developments began replacing sugarcane in the eastern part of the coastal plain in the Ewa area. Additional caprock wells were drilled to provide water to these developments. Since 1988 five new golf courses have been constructed in the Ewa area. Three of these golf courses are irrigated with caprock water from existing sources or from new shallow wells. More housing developments are currently being planned for the Ewa area. The region will be a combination of urban, industrial, and resort land uses.

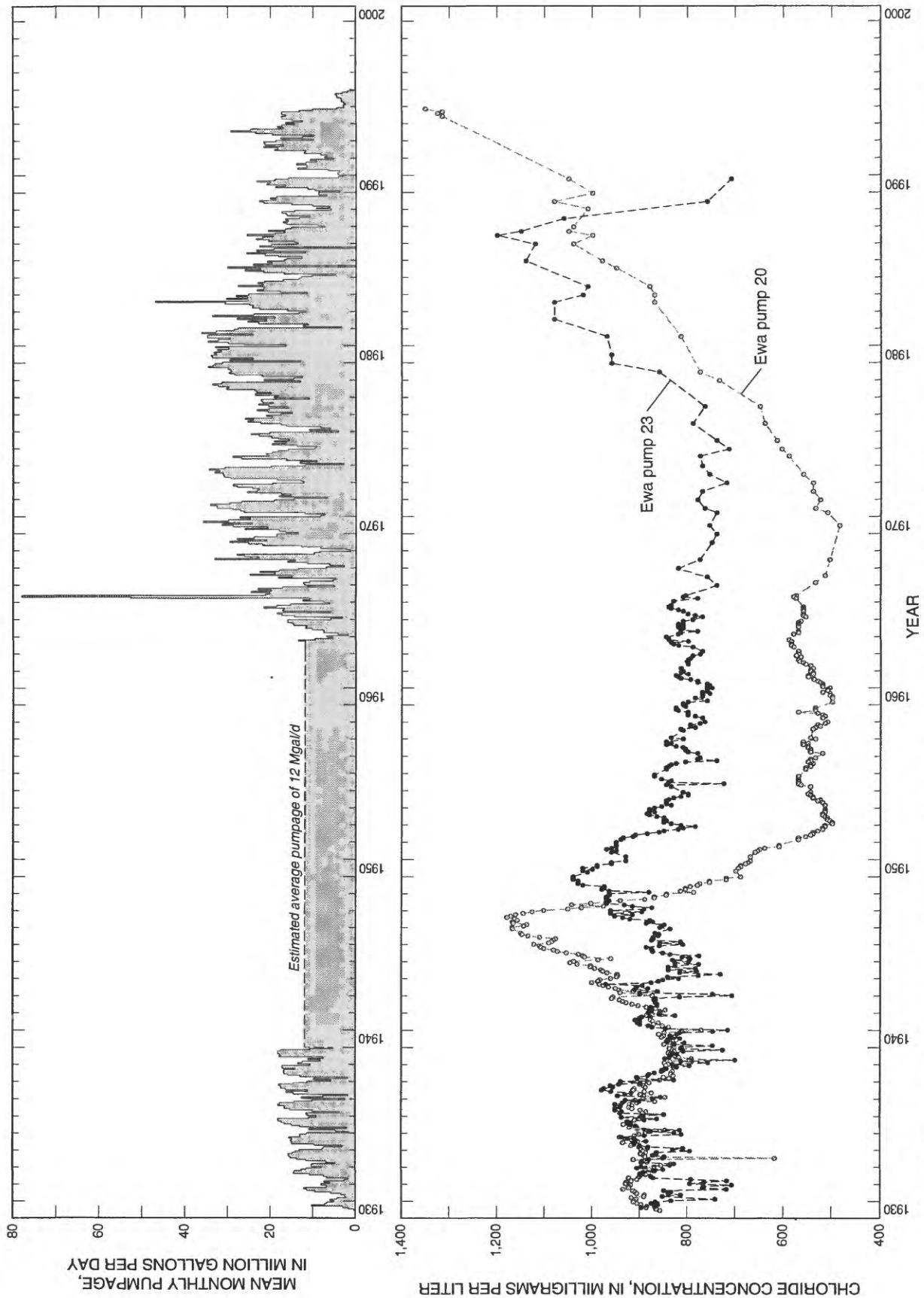

Figure 3. Mean monthly pumpage from the upper limestone unit from wells originally owned by Ewa Plantation and chloride concentrations from water at selected wells in the upper limestone unit of the Ewa caprock (wells shown in fig. 2).

Water quality.--Historically, the quality of water pumped from the volcanic aquifers for irrigation purposes in the Ewa area had an important effect on the quality of shallow ground water in the caprock (Bauer, 1996). Chloride concentration is typically used as an indicator of ground-water quality. Chloride concentrations of water pumped from the volcanic aquifers by Ewa Plantation wells varied with location and time. At Ewa Pumps 1 and 9, for instance, chloride concentrations increased from less than 500 mg/L prior to 1900 to more than 2,500 mg/L during the 1940's. Throughout the pumping history of other Ewa Plantation wells in volcanic rocks, chloride concentrations usually remained less than 1,000 mg/L, and at some wells, less than about 400 mg/L.

A history of chloride concentrations measured at several shallow agricultural wells drilled in the caprock is shown in figure 3. During the 1930's, when Ewa Plantation first began drilling shallow wells in the caprock, chloride concentrations in pumped water typically ranged from about 800 to 1,000 mg/L. Starting in the early 1940's, however, chloride concentrations in caprock wells began rising from about 900 mg/L to more than 1,200 mg/L by 1947 (fig. 3). This increase has been attributed to the use of poor quality irrigation water on sugarcane fields planted over the caprock (Bauer, 1996). The sources of the poor quality irrigation water were deep wells drilled into the volcanic rocks, including Ewa Pumps 1 and 9. After abandoning these two sources, and substituting other fresher sources, water quality in the caprock improved. From 1952 to 1970, chloride concentrations in shallow caprock wells remained relatively steady, ranging from about 500 to 800 mg/L. Bauer (1996) suggests that chloride concentrations began rising in the early 1970's in response to (1) the change from furrow to drip irrigation of sugarcane, (2) increased pumpage from shallow caprock wells, and (3) continued use of poor quality irrigation water on sugarcane fields over the caprock. Sugarcane cultivation ceased in the Ewa area in 1994. However, chloride concentrations continued to rise between 1994 and 1996 after sugarcane cultivation ended.

HYDROGEOLOGIC SETTING

The island of Oahu primarily is formed by the lavas of the older Waianae Volcano to the west and the younger Koolau Volcano to the east. The Waianae and Koolau aquifers are formed by successive, thin-bedded lava flows from the two volcanoes. The Ewa caprock overlies both the Waianae and Koolau volcanic aquifers near the southern coastal ground-water discharge areas (fig. 1).

Volcanic Areas

Geology.--The Waianae and Koolau aquifers have been the subject of many investigations and are described in detail by numerous authors including Stearns and Vaksvik (1935), Wentworth (1951), Visher and Mink (1964), Mink (1980), and Hunt (in press). Lavas of the older Waianae Volcano consist primarily of Waianae Volcanics, while lavas of the younger Koolau Volcano consist primarily of Koolau Basalt (Langenheim and Clague, 1987) (fig. 1). The central saddle area of Oahu was formed by westward flowing Koolau Basalt being deflected northward and southward by the preexisting Waianae Volcano. Koolau Basalt is separated from older Waianae Volcanics by an erosional unconformity.

Ground-water occurrence.--Recharge to the volcanic aquifers is from direct infiltration of rainfall and irrigation return flow over the unconfined parts of the aquifers, and by ground water flowing from upgradient ground-water recharge areas. Fresh ground water in the volcanic aquifers occurs as a freshwater lens floating on denser, underlying saltwater. These lenses are the primary source of fresh ground water on Oahu and are developed by vertical wells and by infiltration tunnels. Within the study area, freshwater lenses exist in both the Waianae and Koolau aquifers. Both aquifers are confined by the caprock near the coast but may be unconfined farther inland. Weathered Waianae Volcanics beneath the erosional unconformity and alluvium form a confining unit between the Waianae aquifer and overlying Koolau aquifer. The confining unit impedes the flow of ground water between the two aquifers.

Freshwater-saltwater flow system.--The main source of freshwater to the flow system in the volcanic rocks is from inland recharge areas. Within the volcanic rocks, freshwater flow is predominantly horizontal between the inland recharge and coastal discharge areas. In the discharge area, freshwater flows from the volcanic rocks into the caprock (see fig. 21).

Saltwater enters the flow system in the volcanic rocks from the ocean by flowing downward through the

caprock. Saltwater within the volcanic rocks also is derived from the ocean from deep circulation in the volcanic rocks. A saltwater circulation system exists beneath the freshwater lens (Souza and Voss, 1987). Saltwater flows landward in the deeper parts of the aquifers, rises, and then mixes with fresher water. This mixing creates a saltwater-freshwater transition zone. The mixed water within the transition zone flows into the caprock.

Water quality.--In general, the chloride concentration in ground water from wells is expected to increase with depth of well, proximity to the coast, and pumping rate. Salinity profiles from deep monitor wells in the Koolau aquifer typically show a three-layered structure (fig. 4). The upper 100 to 300 ft of the lens has a substantial component of local recharge and has a temperature of 20° to 21°C, while the underlying fresher core has a temperature of about 19.5° to 20°C. The freshwater core receives its recharge from the inland, mountainous, high rainfall areas. Beneath the freshwater core of the lens, water temperature increases because of the geothermal gradient. Salinity increases also, ultimately nearing the concentration of seawater in the deeper saltwater flow system of the aquifer.

Water levels.--Within the Koolau aquifer, the first measured (1879) artesian head beneath the caprock was about 32 ft above mean sea level (Thrum, 1889). Within the Waianae aquifer, Mink and others (1988) estimate that the initial head (prior to 1879) in the Ewa area at the coast was about 20 ft above mean sea level. The head difference indicates that ground water initially flowed from the Koolau aquifer into the Waianae aquifer in the Ewa area. The head difference between the aquifers has decreased with time and in recent years has been a few feet. In September 1994 water levels in the Ewa area were 14.86 ft above mean sea level at well 2103-01 in the Waianae aquifer, and 17.89 ft above mean sea level at well 2101-03 in the Koolau aquifer (fig. 2) (Matsuoka and others, 1995). Water levels in both the Koolau and Waianae aquifers typically increase inland at a rate of about 1 ft per mile.

Caprock

Geology.--The surficial geology of the Ewa area as shown by Stearns (1939) and described in detail by George A.L. Yuen and Associates, Inc. (1989) primarily is composed of coralline limestone and younger alluvium (fig. 2). Lithologic logs from U.S. Geological Survey test holes (unpublished data) define the inland extent of the reef limestone that is overlain by alluvium. Detailed geologic logs of wells and test holes (Stearns and Vaksvik, 1938; Stearns and Chamberlain, 1967; Resig, 1969) from several sites in the Ewa area are presented in figure 5. Schematic geologic cross-sections generated from these logs are shown in figure 6.

The volcanic rocks beneath the caprock shown in sections *A-A'* and *B-B'* of figure 6 are part of the Koolau aquifer, while section *C-C'* shows the Waianae aquifer. Geologic logs indicate that the volcanic rocks at the base of the caprock dip seaward about 3 degrees. Near the coast, at well 1959–05, unweathered volcanic rocks lie at a depth of 1,066 ft below mean sea level. At a distance of about 13,000 ft from the coast, at Ewa Plantation wells (2002-01-08,10), unweathered volcanic rocks lie at a depth of about 400 ft below mean sea level.

At the base of the caprock, the volcanic rocks are weathered, and as determined from geologic logs the weathered volcanic rocks are overlain by marine and terrestrial sediments. Near the inland region, where reef limestone is typically absent, thick alluvial deposits overlie the volcanic rocks. Seaward of the mapped alluvium-limestone contact (fig. 2), geologic logs show a thick sequence of interbedded marine and terrestrial sediments of variable thickness that include hard recrystallized reef limestones, marls, calcareous muds, basaltic sands, and terrestrial muds overlying the volcanic rocks. Overlying this sequence is a fossil reef about 50 ft thick (lower limestone unit), which in turn is overlain by an areally extensive 40- to 50-ft thick brown mud (mud unit). This mud consists mainly of clay and silt size particles deposited in a lagoonal environment (Stearns and Chamberlain, 1967). At the top of the section is a 60- to 200-ft thick fossil reef (upper limestone unit).

Ground-water occurrence.--Recharge to the caprock in the Ewa area is from lateral and upward subsurface flow of ground water originating in the volcanic aquifer, and from direct infiltration of rainfall and irrigation return flow (Visher and Mink, 1964). Discharge of ground water from the caprock principally is by subsurface flow to the ocean and by pumping from irrigation wells. Although the entire Ewa caprock is saturated with ground water below the water table, only the upper limestone unit has been extensively developed as a source of ground water. The upper limestone unit is an

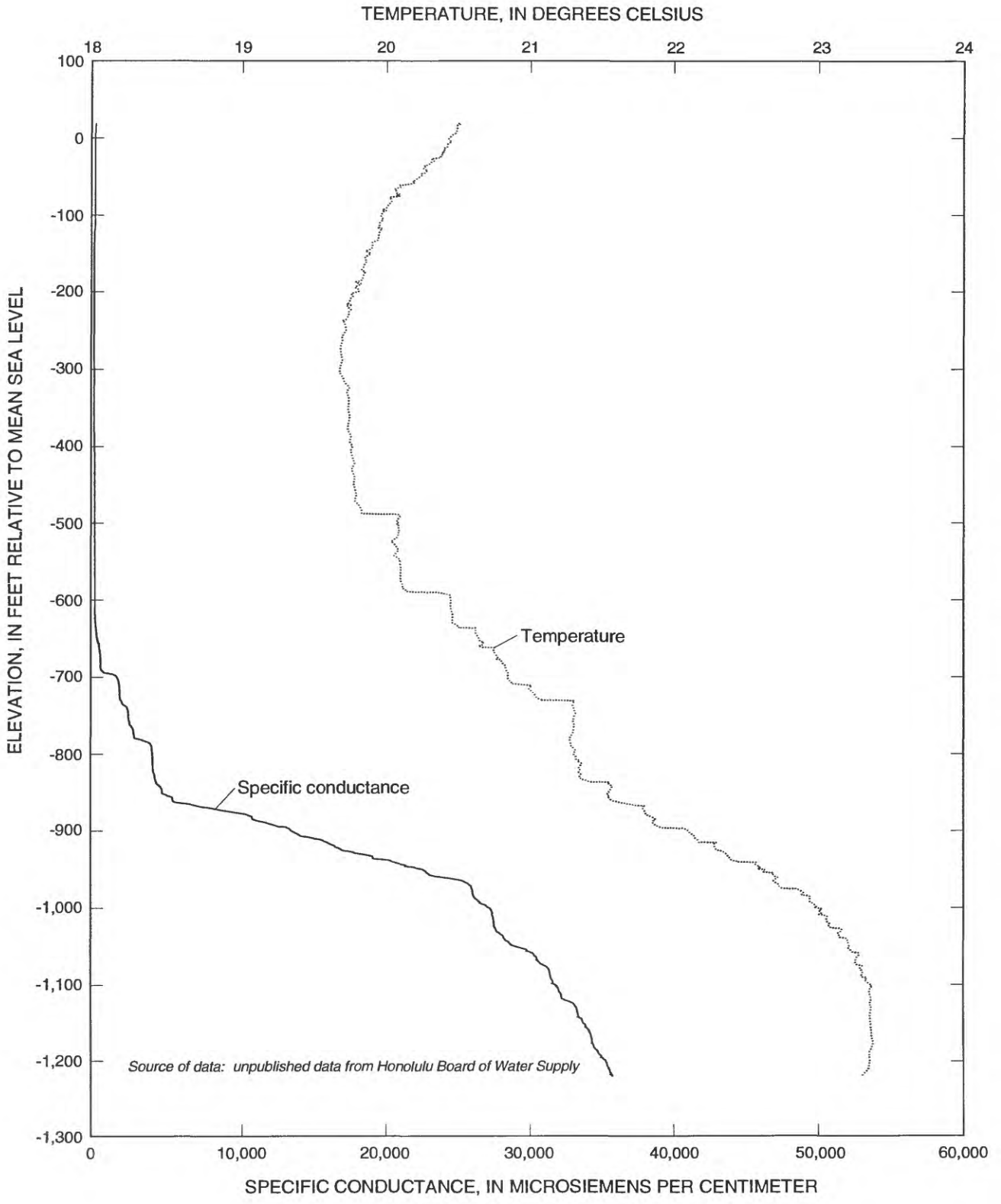

Figure 4. Specific conductance and temperature profiles of April 23, 1987 for Waipio deep monitor well 2659-01, Oahu, Hawaii (well shown in fig. 1).

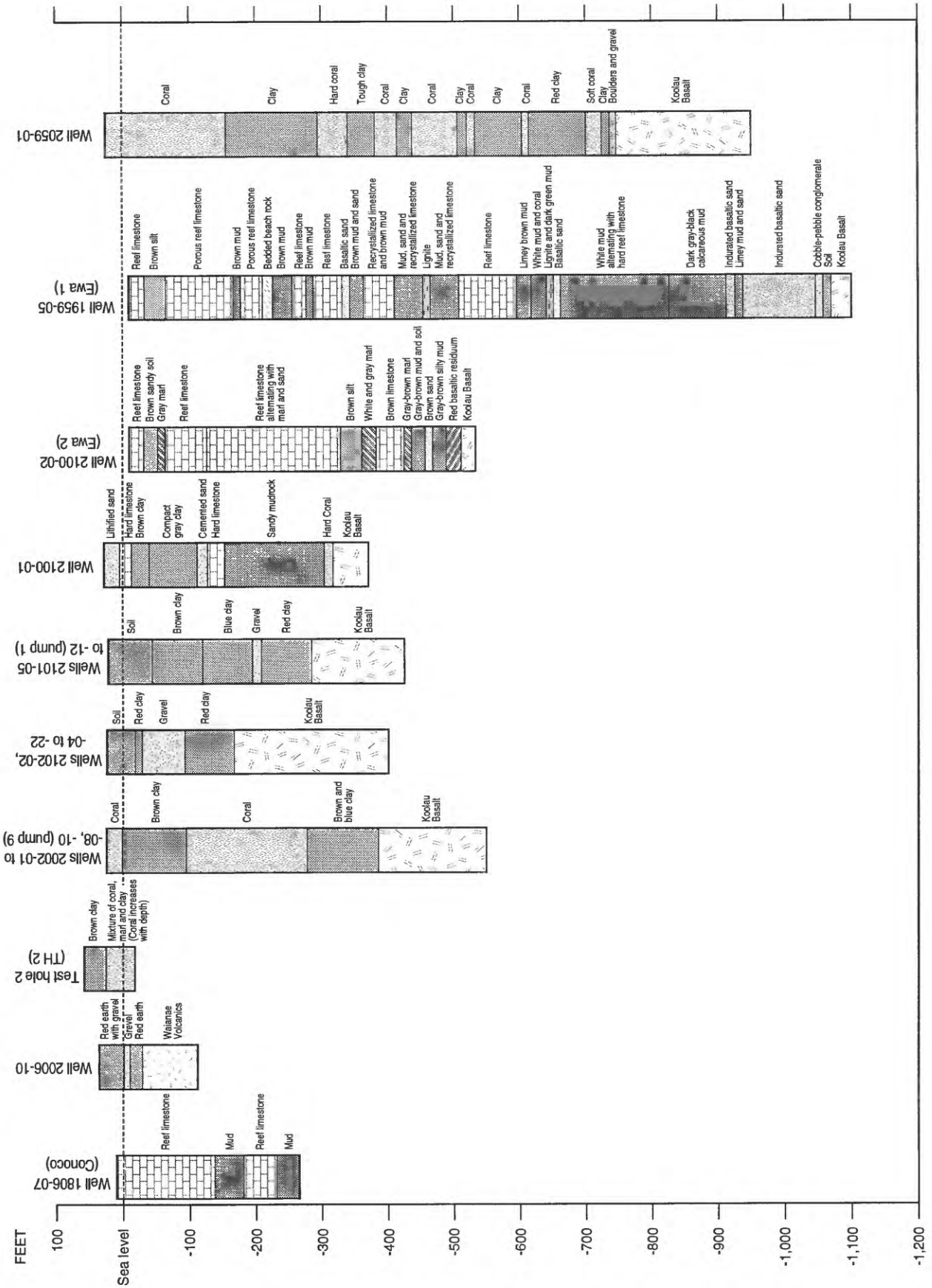

Figure 5. Geologic logs from selected wells in the Ewa area, Oahu, Hawaii.

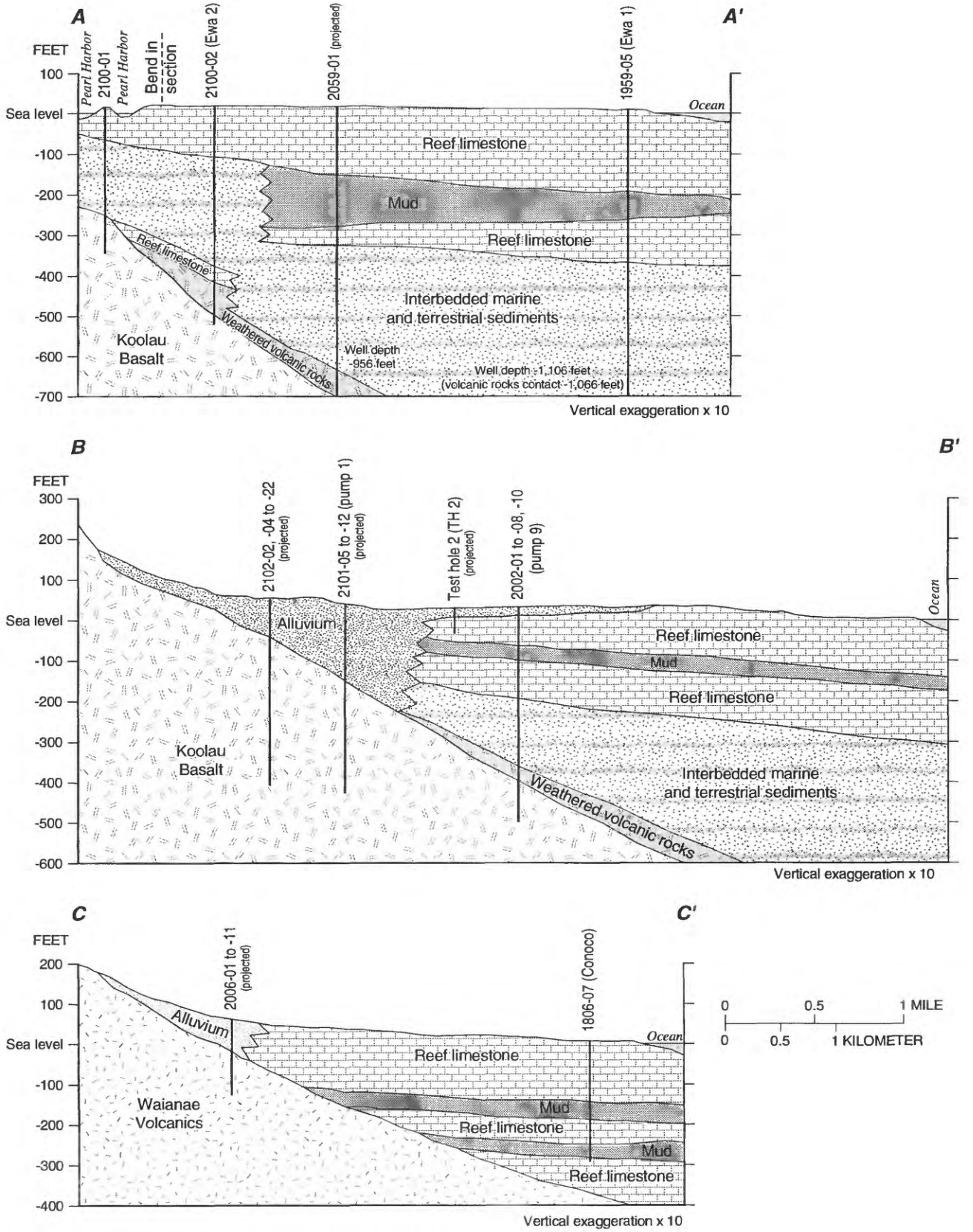

Figure 6. Schematic cross sections of the Ewa area, Oahu, Hawaii (trace of sections shown in figure 2).

unconfined aquifer where it is not overlain by alluvium near sea level. The 40- to 50-ft thick mud unit described earlier underlies the upper limestone unit.

Water quality.--The upper limestone unit contains brackish water which historically has been used for irrigation purposes. Stearns and Vaksvik (1935) concluded that ground water in the upper limestone unit primarily is from return irrigation water from alluvial lands that are inland of and at a higher elevation than the exposed limestone. Freshwater used to irrigate these lands was supplied by artesian wells in the volcanic aquifer.

The existence of a freshwater-saltwater flow system in the upper limestone unit is indicated by recent salinity profiles (Tom Nance Water Resources Engineering and Mackle Martin and Associates Pty, Ltd., 1991; Nance and McNulty, 1993) as well as resistivity profiles (Cox and Lao, 1967) from wells in the Ewa area. Vertical salinity profiles for a well near the coast and a well about 2 miles from the coast are shown in figure 7. The salinity profiles in figure 7 indicate a thin lens underlain by saltwater in the upper limestone unit close to shore. Other investigators (Lau and others, 1986), have reported chloride concentrations within a narrow range from 234 to 490 mg/L in a profile of a well (fig. 2, UH well N), which was screened throughout the upper limestone unit and which terminated at the top of the underlying mud unit at an elevation of 80 ft below mean sea level.

The salinity distribution in the deeper sections of the caprock cannot be fully characterized because of a lack of data below the upper limestone unit. Data from a few wells drilled in the western part of the caprock, however, indicate that the lower limestone unit contains highly brackish ground water (unpub. data, Hawaii Commission on Water Resource Management well files).

Water levels.--Within the upper limestone unit of the caprock, ground-water levels range from a few tenths of feet above mean sea level near the coast to 1 to 3 ft above mean sea level over most of the inland study area. Within the upper limestone unit, water levels are strongly influenced by ocean tides. Reported tidal efficiencies exceed 90 percent within a few hundred feet of the coast and may be greater than 50 percent at a distance of 2,000 ft inland from the coast (Nance and McNulty, 1993). For typical daily tidal fluctuations of about 1 to 2 ft, corresponding ground-water level fluctuations may exceed 0.5 to 1 ft at a distance of 2,000 ft inland from the coast.

Estimates of Hydraulic Conductivity

Unweathered volcanic rocks.--On the scale of a core sample, hydraulic conductivity measurements for unweathered volcanic rocks of Oahu are as low as 3.5×10^{-5} ft/d (Ishizaki and others, 1967). Local-scale aquifer tests conducted on Oahu indicate a range of hydraulic conductivities from tens of feet per day to tens of thousands of feet per day (Soroos, 1973). On a regional scale, however, the range of estimates for the horizontal hydraulic conductivity of volcanic rocks of Oahu is much narrower, ranging from about 1,000 ft/d to about 5,000 ft/d (Mink, 1980; Mink and Lau, 1980; Souza and Voss, 1987).

Weathered volcanic rocks.--Weathered volcanic rocks may have a much lower permeability relative to unweathered volcanic rocks depending on the extent of weathering. Using cores samples, Wentworth (1938) estimated the hydraulic conductivity of weathered basalt to be from 0.083 to 0.128 ft/d. Miller (1987) estimated the saturated hydraulic conductivity of saprolite core samples collected beneath pineapple fields of central Oahu to be between 0.0028 and 283 ft/d.

Alluvium.--The hydraulic conductivity of alluvium is highly variable depending on the extent of compaction and weathering. Wentworth (1938) estimated the hydraulic conductivity of alluvium and weathered alluvium core samples to range from about 0.01 ft/d to 1.0 ft/d.

Limestone.--Previous studies of the Ewa area have produced a range of estimates for the hydraulic conductivity of the upper limestone unit. Dale (1968; in George A.L. Yuen and Associates, Inc., 1989, p. 31), and later Williams (1976), used tidal response data from wells to calculate the hydraulic conductivity in the upper limestone unit during the planning and construction of the Barbers Point Deep Draft Harbor (fig. 2). Dale calculated a hydraulic conductivity of 33,000 ft/d, whereas Williams computed a value of 20,822 ft/d. George A.L. Yuen and Associates, Inc. (1989, p. 31–32) and Lau and others (1989, p. 19–20) suggest that these hydraulic conductivity values are high for a regional estimate because total caprock outflow computed using these values in conjunction with measured hydraulic gradients would be much greater than esti-

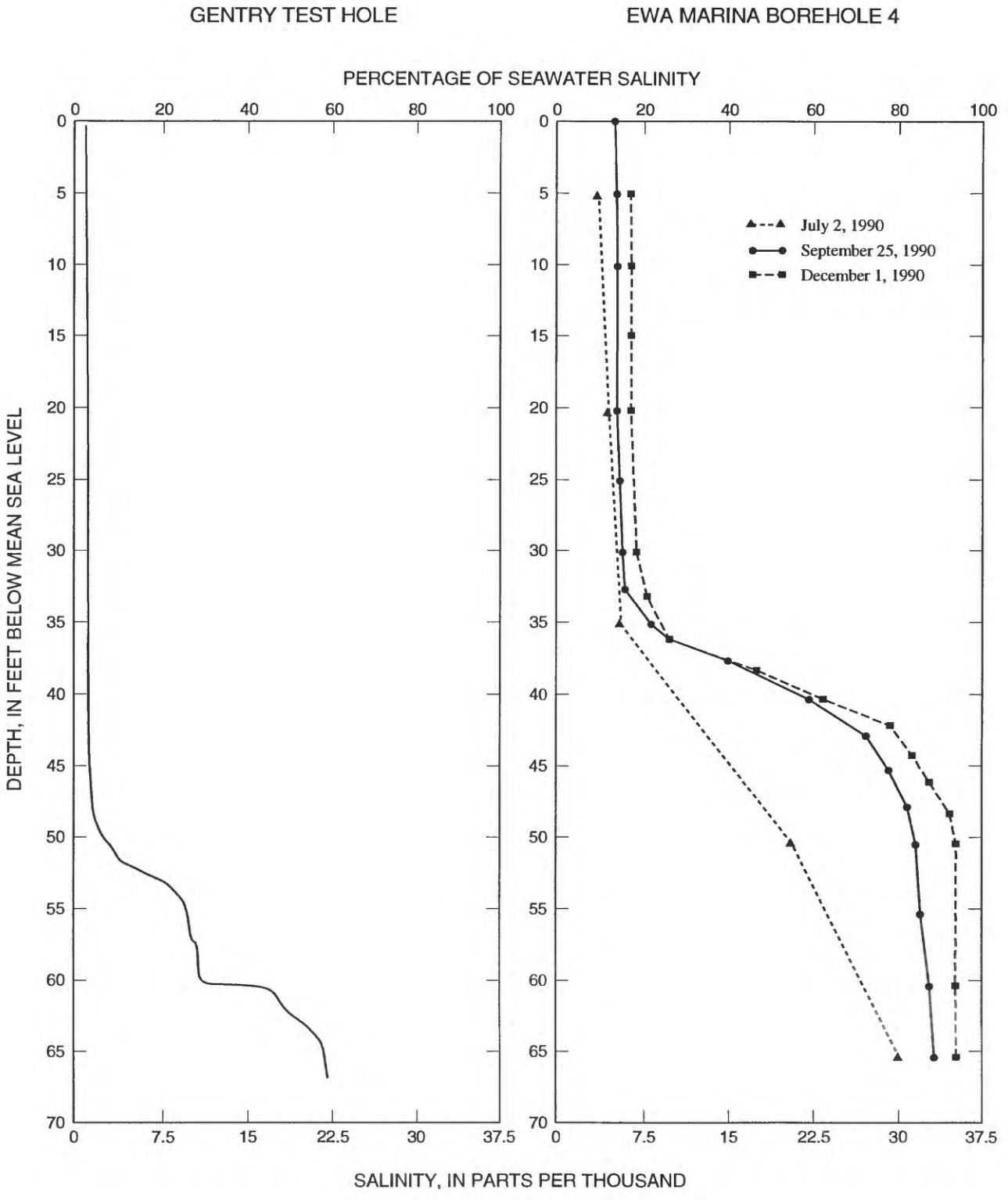

Figure 7. Vertical salinity profiles from two wells in the upper limestone unit of the Ewa caprock, Oahu, Hawaii (Gentry test hole profile modified from Nance and McNulty, 1993; Ewa Marina borehole 4 profile modified from Tom Nance Water Resources Engineering and Mackle Martin and Associates Pty Ltd., 1991) (wells shown in fig. 2).

mates from a hydrologic balance. George A.L. Yuen and Associates, Inc. estimate the hydraulic conductivity of the limestone to be 2,500 ft/d. Camp Dresser and McKee (1993a) summarize existing hydraulic conductivity estimates from tidal analyses and aquifer tests. Reported hydraulic conductivity estimates range from 25 to 30,000 ft/d from tidal analyses, and 2 to 12,400 ft/d from aquifer tests.

Tom Nance Water Resource Engineering and Mackle Martin and Associates (1991) constructed a two-dimensional, sharp interface, ground-water flow model for the upper limestone unit of the coastal plain in the Ewa area. Using tidal response data, the hydraulic conductivity for most of the upper limestone was estimated to be 25,000 ft/d inland of the coast. Camp Dresser and McKee (1993b) simulated flow in the upper limestone layer using a three-dimensional, sharp interface, ground-water flow model. The horizontal and vertical components of hydraulic conductivity for the upper limestone layer obtained by model calibration were 5,600 and 13 ft/d, respectively.

NUMERICAL MODEL

In this study, a cross-sectional ground-water model of the Ewa area was developed to identify the major hydrogeologic controls on the regional movement of ground water and the salinity distribution within the caprock. The finite element computer code SUTRA (Voss, 1984) simulates two-dimensional, density-dependent flow and solute transport and was used in this study to generate steady-state pressures and solute concentrations for each hydraulic conductivity distribution tested. Solute concentrations in the model are expressed as a mass fraction of kg of total dissolved solids (TDS) per kg of fluid (kg/kg). In the model, 100 percent seawater salinity has a TDS concentration of 0.0357 kg/kg.

Data are unavailable to describe the pressure and salinity distributions in the deeper caprock and, thus, no attempt was made to calibrate the model. Instead, the model was used as a tool to develop a refined conceptual model of the ground-water flow system in the Ewa caprock by simulating a series of scenarios using reasonable distributions of hydraulic conductivity and a generalized caprock stratigraphy. Because the model was not calibrated, the model-calculated water level and salinity distributions should not be construed to represent actual field conditions. In addition, the actual amount of subsurface inflow from the volcanic rocks to the caprock cannot be determined without a calibrated model.

Model grid

The modeled section is located along section *B-B'* (fig. 6) near the center of the coastal plain in the Ewa area. The modeled section is 48,000 ft in length and extends about 1,000 ft inland from cross-section endpoint *B* and about 20,000 ft seaward of endpoint *B'*. Relative to the geologic section, the modeled section was extended in depth from 600 ft to 5,000 ft below mean sea level to an approximate aquifer bottom (Souza and Voss, 1987).

The finite element mesh consists of 3,250 nodes, arranged in a rectangular 50 by 65 array, and 3,136 elements (fig. 8). Node spacing is variable. Discretization is finest where hydraulic and concentration gradients are expected to be steep. Horizontally, node spacing varies from 100 ft near the coast to 5,000 ft at the seaward boundary. Vertically, the node spacing varies from 10 ft in the upper 300 ft of the section to 2,000 ft at the bottom. The modeled section has an arbitrary width of 3.28 ft. All modeled flow rates are normalized and reported as Mgal/d per mile of cross-sectional width.

For modeling purposes, the generalized geologic section includes unweathered volcanic rocks and the Ewa caprock. The heterogeneous Ewa caprock stratigraphy was divided into six zones (fig. 9): (1) upper limestone layer; (2) lower limestone layer; (3) mud layer between the upper and lower limestone; (4) upper alluvium; (5) interbedded marine and terrestrial sediments; and (6) weathered volcanic rocks. The terms ***zone*** and ***layer*** are used to describe model stratigraphy. The model ***zones*** and ***layers*** correspond to geologic ***units*** described in the previous sections.

Boundary Conditions

The boundary conditions for the cross-sectional model are shown schematically in figure 8. The inland, vertical boundary consists of a specified, 17-ft hydrostatic freshwater pressure condition along the upper 33 nodes (340 ft) and a no-flow condition along the lower 32 nodes. Freshwater may enter the modeled system from the upper 33 nodes of the inland, vertical bound-

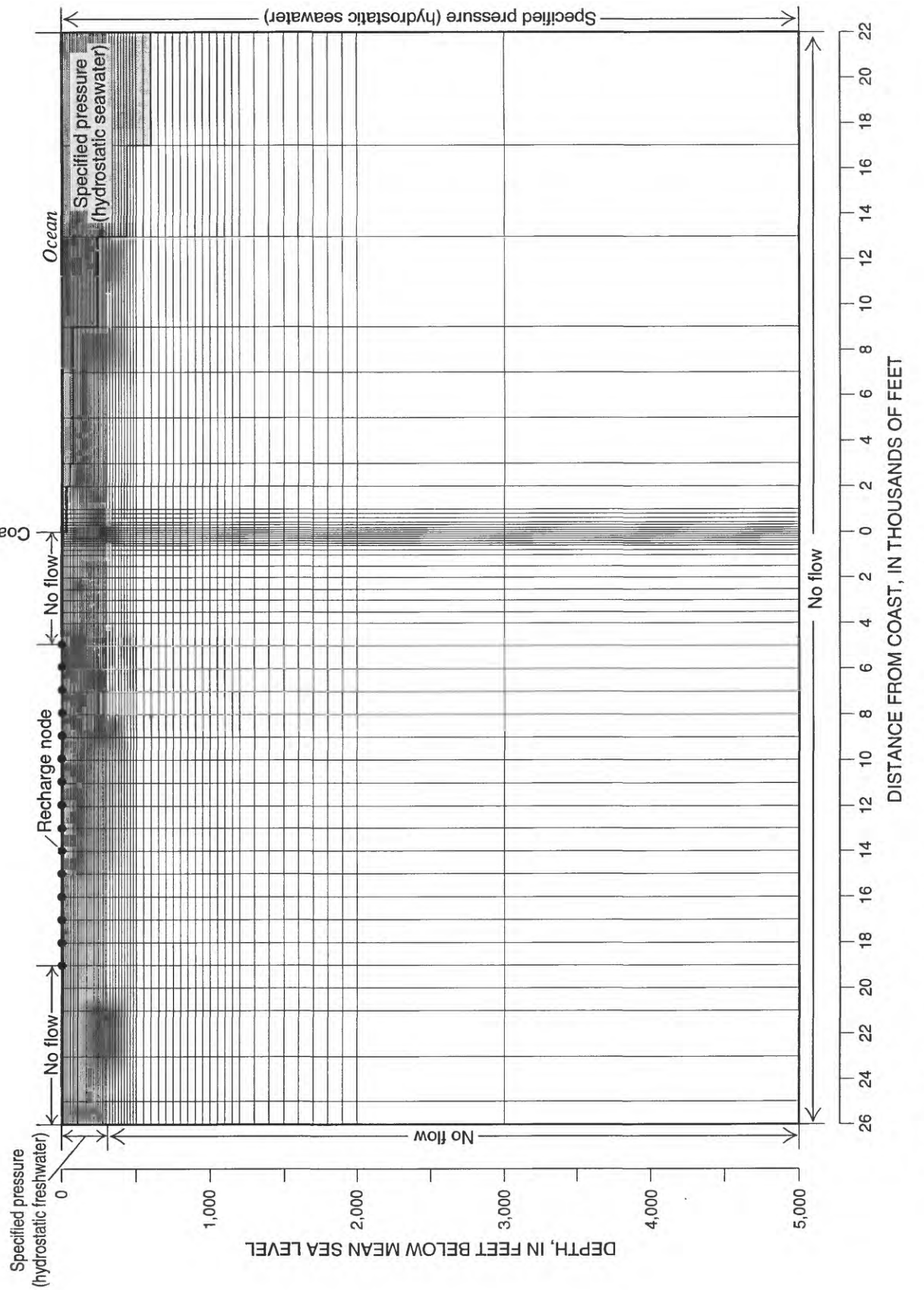

Figure 8. Finite-element mesh and boundary conditions for Ewa vertical cross-sectional model.

ary. (The amount of freshwater inflow at this boundary and the salinity distribution in the volcanic rocks were not significantly affected by the depth of this specified pressure condition.) The effects on freshwater inflow at this specified pressure boundary are discussed in the "Model Results" section. The bottom boundary is a no-flow boundary. Along the seaward vertical boundary and within the ocean, a specified hydrostatic seawater pressure condition is used. The top boundary consists of a specified zero-pressure condition offshore, and a no-flow condition onshore except where inflow is specified at recharge nodes (fig. 8).

In the model simulations, solute transport at boundaries is dependent on whether ground-water is flowing into or out of the mesh at model boundaries. At nodes where ground-water inflow is specified, the TDS concentration of the inflow is specified. At the inland, vertical boundary, the TDS concentration of inflow from the upper 33 nodes is 0.1 percent that of seawater (corresponding to a typical chloride concentration in freshwater of 20 mg/L). Fluid entering the model at recharge nodes along the top, onshore boundary has a TDS concentration of 1.0 percent that of seawater (corresponding to an arbitrary chloride concentration of 200 mg/L). At all offshore specified pressure nodes, inflow has a TDS concentration of 100 percent that of seawater. All flow out of the model section, either at specified discharge nodes or specified pressure nodes, has a TDS concentration corresponding to the ambient concentration of the fluid in the aquifer.

Recharge

Ground-water recharge is a function of several factors including (1) water available from rainfall and irrigation, (2) land use, (3) soil type, and (4) evapotranspiration rate. For this study, recharge was computed from estimates by Giambelluca (1986). The land-use classes used in this study include furrow-irrigated sugarcane, low-density urban, and natural cover. For an average annual rainfall rate of about 19.7 in., Giambelluca estimated the average annual recharge rate for each of the relevant land uses (table 1).

Two land-use distributions were considered for this study, one without sugarcane and one with sugarcane using furrow irrigation.

Without sugarcane.--For this land-use distribution, 75 percent of the area was considered to be under natural cover and 25 percent of the area was considered to be low-density urban; the area-weighted average recharge is 3.3 in/yr.

With sugarcane.--For this land-use distribution, 75 percent of the area was considered to be furrow-irrigated sugarcane and the remaining 25 percent of the area was treated as low-density urban; the area-weighted average recharge is 63 in/yr.

For both land-use distributions, recharge was distributed evenly to 15 nodes, representing 15,000 ft of length, along the top boundary of the caprock (fig. 8). Accordingly, recharge rates of 63 and 3.3 in/yr represent flow rates of 8.5 and 0.45 Mgal/d per mile of cross-sectional width, respectively.

Inflow from Volcanic Rocks

Subsurface inflow from the volcanic aquifer into the caprock at the inland boundary is largely unknown. Using a chemical mass-balance mixing model, George A.L. Yuen and Associates, Inc. (1989) estimated total upward flow from the volcanic rocks at the inland part of the caprock to be about 4 to 5 Mgal/d. If the inflow zone is assumed to be about 4 mi wide, the estimated rate of inflow from the volcanic rocks is about 1.0 to 1.25 Mgal/d per mile of cross-sectional width. Camp Dresser and McKee (1994) assumed a value of 1.25 Mgal/d per mile of cross-sectional width in their model of the upper limestone layer.

Because of the uncertainty in subsurface inflow into the caprock, inflow from the volcanic rocks was simulated by assigning a specified-pressure boundary condition at the inland vertical boundary of the model section. By using this boundary condition, inflow from the volcanic rocks is determined by the model depending on the hydraulic conductivity distribution, recharge, and pumping rates assigned in the model. The specified-pressure condition at this boundary corresponds to a constant 17-ft head in the volcanic aquifer. Use of this

Table 1. Ewa ground-water recharge rates by land-use class, Oahu, Hawaii

[Recharge values are from Giambelluca, 1986; the recharge values correspond to a rainfall rate of 19.7 inches per year]

Land use	Recharge (inches per year)
Sugarcane, furrow-irrigated	83.8
Low-density urban	1.5
Natural cover	3.9

boundary condition assumes that the water levels in the volcanic rocks at the boundary are unaffected by changes in hydraulic conductivity, caprock stratigraphy, recharge, or pumpage.

Pumpage

Two caprock pumpage distributions were used in this study, corresponding to the two recharge distributions described in a previous section. Caprock pumpage was assumed to be zero in all simulations with an assumed caprock recharge of 0.45 Mgal/d per mile of cross-sectional width (non-irrigation). Caprock pumpage was assumed to be 4 Mgal/d per mile of cross-sectional width in all simulations with an assumed caprock recharge of 8.5 Mgal/d per mile of cross-sectional width (furrow-irrigation). Caprock pumpage was distributed evenly to 18 pumping nodes (fig. 9). The effects of pumping from the volcanic aquifer were not considered in this study.

Dispersivity

SUTRA approximates the mixing between saltwater and freshwater by assuming that the dispersive process is controlled by the salinity concentration gradient, the ground-water velocity, and an aquifer dispersivity parameter (Voss, 1984). Dispersion may occur in both the longitudinal and transverse directions relative to the direction of ground-water flow. In layered systems, the length scale of the permeability structure is much larger parallel to layering than across it. Thus, the effective longitudinal dispersivity need not have the same value for flow parallel to layers and perpendicular to layers (Silliman and others, 1987; Fattah and Hoopes, 1985). Further, transverse dispersivity may not have the same value for flow parallel to layers and perpendicular to layers (Fattah and Hoopes, 1985). SUTRA uses an anisotropic dispersion model which accounts for direction-dependent longitudinal and transverse dispersivities.

A summary of the dispersivity values used is shown in table 2. Souza and Voss (1987) estimated the longitudinal dispersivity for unweathered volcanic rocks to be about 250 ft. An anisotropic dispersion model was used for longitudinal dispersivity in the limestone layers. For these layers the length scale of the permeability structure is expected to be larger in the horizontal direction (parallel to the layering) than in the vertical direction (perpendicular to the layering). For the limestone layers, the maximum (horizontal) longitudinal dispersivity was assumed to be 250 ft. (Sensitivity analysis showed that the model-calculated salinity distribution is not significantly affected by the maximum longitudinal dispersivity within the plausible range of 50 to 500 ft.) Within the limestone layers, the ratio of the maximum to minimum longitudinal dispersivity was assumed to be the same as the assigned ratio of horizontal to vertical hydraulic conductivity of 10:1. Thus, the minimum longitudinal dispersivity for these layers was assigned a value of 25 ft. For the upper alluvium, mud layer, interbedded marine and terrestrial sediments, and weathered volcanic rocks, the maximum and minimum longitudinal dispersivities were assumed to be 10 ft.

Table 2. Model dispersivity values used in scenarios 1 through 10, Ewa, Oahu, Hawaii

Model zone	Longitudinal dispersivity (in feet)		Transverse dispersivity (in feet)	
	Maximum	Minimum	Maximum	Minimum
Upper limestone layer	250	25	1	1
Mud layer	10	10	1	1
Lower limestone layer	250	25	1	1
Upper alluvium, marine and terrestrial sediments, and weathered volcanic rocks	10	10	1	1
Unweathered volcanic rocks	250	250	1	1

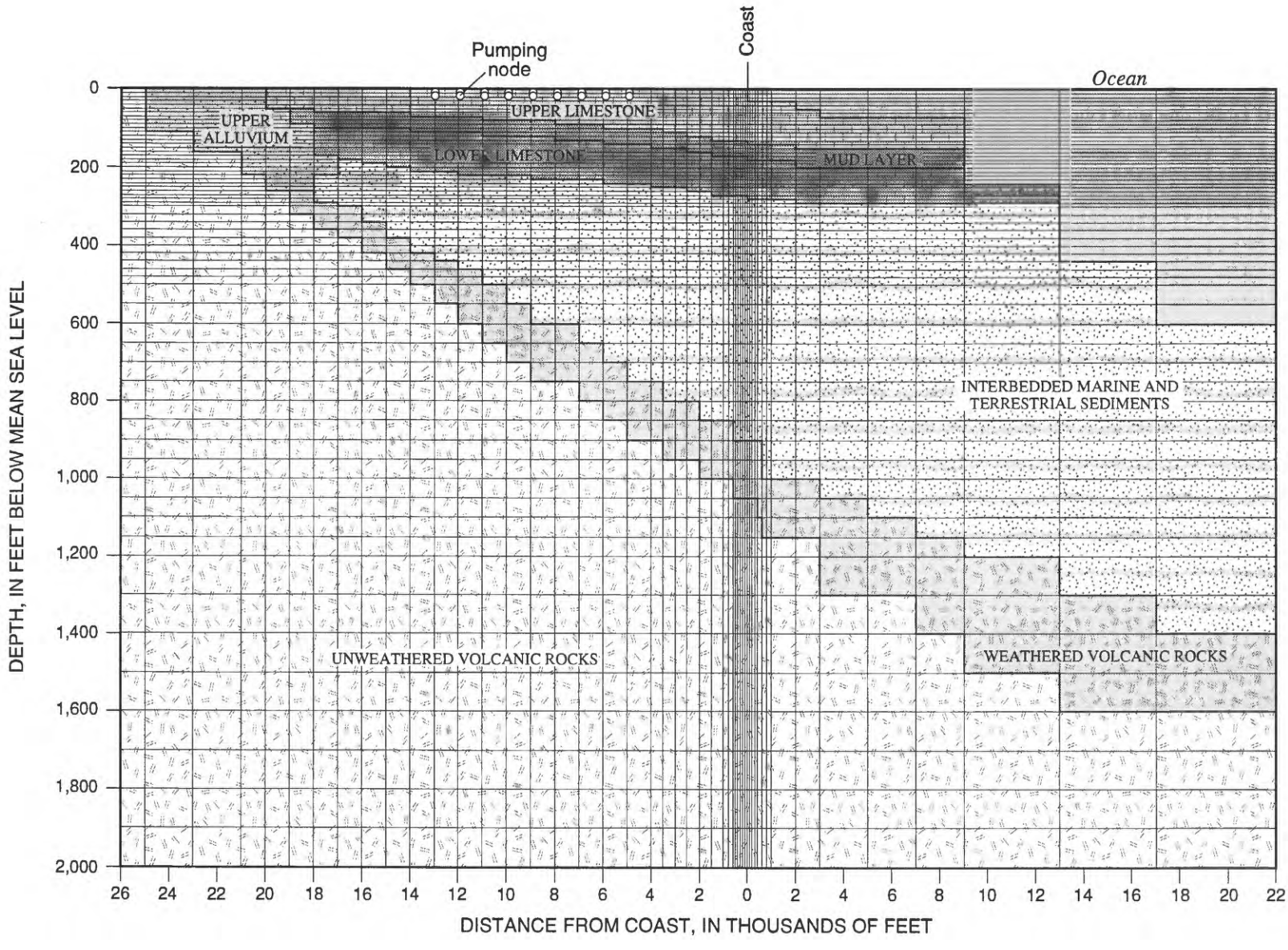

Figure 9. Generalized caprock zones and pumping nodes for Ewa vertical cross-sectional model.

Transverse dispersivity is typically less well known than longitudinal dispersivity. For cross-sectional transport in systems with anisotropic permeability, transverse dispersivity may be less than one-hundredth of longitudinal dispersivity for flows along the maximum permeability direction (Gelhar and Axness, 1983). Souza and Voss (1987) estimated the transverse dispersivity for unweathered volcanic rocks to be about 1 ft. Published dispersivity estimates for the caprock units overlying the volcanic rocks, however, are unavailable. For all caprock zones, transverse dispersivities were assigned values of 1 ft.

DESCRIPTION OF MODEL SCENARIOS

The cross-sectional model was used to evaluate, with steady-state simulations, the controls that affect ground-water flow and salinity distribution within the Ewa caprock. Controls considered were: (1) overall caprock hydraulic conductivity, (2) hydraulic conductivity of the mud layer, (3) hydraulic conductivity of the upper limestone layer, and (4) layered heterogeneity within the upper limestone. In addition, the possible effects of changes in recharge as a result of irrigation practices, and the effects of a marina excavation were evaluated. A summary of the hydraulic conductivity values assigned to each zone is shown in table 3 for each of the ten scenarios described in this report. The horizontal and vertical components of hydraulic conductivity for unweathered volcanic rocks were assumed to be 1,500 and 7.5 ft/d, respectively (Souza and Voss, 1987); these values were held constant for all simulations. A brief description of each scenario is presented below.

Scenario 1. --This scenario represents an initial estimate of the regional hydraulic conductivity from published values. Horizontal and vertical hydraulic conductivities of 3,000 and 300 ft/d, respectively, were used for both the upper and lower limestone layers. All other caprock zones were assigned an isotropic hydraulic conductivity of 0.1 ft/d; this value is consistent with previous estimates of the overall hydraulic conductivity for the caprock (Souza and Voss, 1987). Caprock recharge and pumpage were assumed to be 0.45 and 0 Mgal/d per mile of cross-sectional width, respectively (non-irrigation). These recharge and pumping rates were also used in scenarios 2 through 6, and scenarios 8 through 10.

Scenario 2.--This scenario increases only the isotropic hydraulic conductivities of the upper alluvium, marine and terrestrial sediments, and weathered volcanic rock zones by an order of magnitude relative to scenario 1. Because these zones form the bulk of the caprock, this change increases the overall hydraulic conductivity of the caprock. For these zones, the isotropic hydraulic conductivity was increased to 1.0 ft/d.

Scenario 3.--This scenario reduces only the isotropic hydraulic conductivities of the upper alluvium, marine and terrestrial sediments, and weathered volcanic rock zones by an order of magnitude relative to scenario 1, and reduces the overall hydraulic conductivity of the caprock. For these zones, the isotropic hydraulic conductivity was reduced to 0.01 ft/d.

Scenario 4.--This scenario reduces only the isotropic hydraulic conductivity of the mud layer by two orders of magnitude relative to scenario 1. In scenario 1, the hydraulic conductivity of the mud layer was assigned the same value as that previously estimated for the overall caprock. However, the mud layer has been treated as a confining unit (for example, Camp Dresser and McKee, 1994) and may have a lower hydraulic conductivity. The isotropic hydraulic conductivity of the mud layer in scenario 4 was reduced to 0.001 ft/d.

Scenario 5.--This scenario divides the upper limestone layer into upper and lower sublayers to represent layered heterogeneity. The top 20 ft of the upper limestone layer was assigned horizontal and vertical hydraulic conductivities of 30,000 and 3,000 ft/d, respectively. The lower part of the upper limestone layer and the remaining zones of the caprock are identical to scenario 1.

Scenario 6.--This scenario divides the upper limestone layer into upper and lower sublayers to represent layered heterogeneity which differs from scenario 5. The top 50 ft of the upper limestone layer was assigned horizontal and vertical hydraulic conductivities of 300 and 30 ft/d, respectively. The lower part of the upper limestone layer was assigned horizontal and vertical hydraulic conductivities of 30,000 and 3,000 ft/d, respectively. The remaining zones of the caprock are identical to scenario 1.

Scenario 7. --This scenario increases caprock recharge from 0.45 to 8.5 Mgal/d per mile of cross-sectional width (to represent recharge from furrow irrigated sugarcane), and pumpage from 0 to 4 Mgal/d per mile of cross-sectional width (to represent pumping for

Table 3. Assigned hydraulic conductivity values, in feet per day, by scenario and model zone, Ewa, Oahu, Hawaii

Scenario no.	Upper limestone layer		Mud layer		Lower limestone layer		Upper alluvium, marine and terrestrial sediments, and weathered volcanic rocks		Unweathered volcanic rocks	
	horizontal	vertical	horizontal	vertical	horizontal	vertical	horizontal	vertical	horizontal	vertical
1	3,000	300	0.1	0.1	3,000	300	0.1	0.1	1,500	7.5
2	3,000	300	0.1	0.1	3,000	300	1.0	1.0	1,500	7.5
3	3,000	300	0.1	0.1	3,000	300	0.01	0.01	1,500	7.5
4	3,000	300	0.001	0.001	3,000	300	0.1	0.1	1,500	7.5
5	30,000[a], and 3,000[b]	3,000[a], and 300[b]	0.1	0.1	3,000	300	0.1	0.1	1,500	7.5
6	300[c], and 30,000[d]	30[c], and 3,000[d]	0.1	0.1	3,000	300	0.1	0.1	1,500	7.5
7	3,000	300	0.1	0.1	3,000	300	0.1	0.1	1,500	7.5
8	3,000	300	0.1	0.1	3,000	300	0.01	0.01	1,500	7.5
9	3,000	300	0.001	0.001	3,000	300	0.1	0.1	1,500	7.5
10	30,000[a], and 3,000[b]	3,000[a], and 300[b]	0.1	0.1	3,000	300	0.1	0.1	1,500	7.5

[a]top 20 ft of upper limestone layer
[b]upper limestone sublayer, below the top 20 ft
[c]top 50 ft of upper limestone layer
[d]upper limestone sublayer, below the top 50 ft

sugarcane irrigation). The hydraulic conductivity distribution in this scenario is identical to the hydraulic conductivity distribution of scenario 1.

Scenario 8.-- This scenario modifies the geometry of the upper limestone layer at the modeled shoreline. This modification represents a marina excavation 20 ft deep extending 1,500 ft inland from the coast. The hydraulic conductivity distribution used in this scenario is identical to that of scenario 3 except in the vicinity of the simulated marina excavation, where a part of the upper limestone layer is removed.

Scenario 9.-- This scenario uses the same marina excavation modification described in scenario 8. The hydraulic conductivity distribution used in this scenario is identical to that of scenario 4 except in the vicinity of the simulated marina excavation, where a part of the upper limestone layer is removed.

Scenario 10.-- This scenario uses the same marina excavation modification described in scenario 8. The hydraulic conductivity distribution used in this scenario is identical to that of scenario 5 except in the vicinity of the simulated marina excavation, where a part of the upper limestone layer is removed.

MODEL RESULTS

The effects of various hydraulic conductivity and recharge distributions represented by the different scenarios were evaluated by examining model-calculated water level and salinity distributions. Salinity concentrations computed by the model were divided by the assumed salinity of seawater to obtain concentrations in percentage of seawater salinity. Specifically, results of the various scenarios were compared on the basis of model-calculated (1) water levels in the upper limestone, (2) salinity distribution throughout the caprock, (3) ground-water flow through the mud layer, and (4) inflow from volcanic rocks to the caprock.

Generalized Flow System - Scenario 1

In scenario 1, an initial distribution of hydraulic conductivity for the volcanic rocks and caprock was assigned on the basis of published values. It should be noted that scenario 1 does not represent a calibrated model, nor does it represent a best estimate of the hydraulic conductivity distribution for the caprock. Rather, scenario 1 is used as a basis for comparison with other scenarios. Consequently, results from this scenario are presented in detail below. The model-calculated water levels and salinity distribution for scenario 1 are shown in figure 10. Results of scenario 1 are representative of the general ground-water flow pattern in the volcanic rocks and caprock.

Inflow from volcanic rocks.--Inflow of fresh ground water from the volcanic aquifer to the caprock is simulated in the model by assigning a specified-pressure condition at the inland boundary of the mesh. In all scenarios, the head in the volcanic rocks at the inland boundary was assumed to be 17 ft for the top 340 ft of the aquifer. The rate of inflow is computed by the model and is dependent on the hydraulic conductivity distribution, recharge, and pumping rates assigned in the model. A summary of the ground-water inflow values from the volcanic rocks for scenario 1 and all other scenarios is presented in table 4. For scenario 1, the model-calculated inflow of fresh ground water from the volcanic aquifer is about 1.6 Mgal/d per mile of cross-sectional width.

Table 4. Simulated Inflow from the volcanic rocks, Ewa, Oahu, Hawaii
[Mgal/d, million gallons per day]

Scenario no.	Inflow (Mgal/d per mile of cross section width)
1	1.6
2	5.3
3	0.2
4	1.2
5	1.7
6	1.6
7	1.3
8	0.2
9	1.2
10	1.7

Transition zone in volcanic rocks.--The transition zone in the volcanic rocks near the base of the caprock controls the distribution of salinity of water flowing into the caprock. The model-calculated transition zone in the volcanic rocks is shown in figure 10B. The thickness of this transition zone is consistent with observed data as well as the modeled transition zone of Souza and Voss (1987).

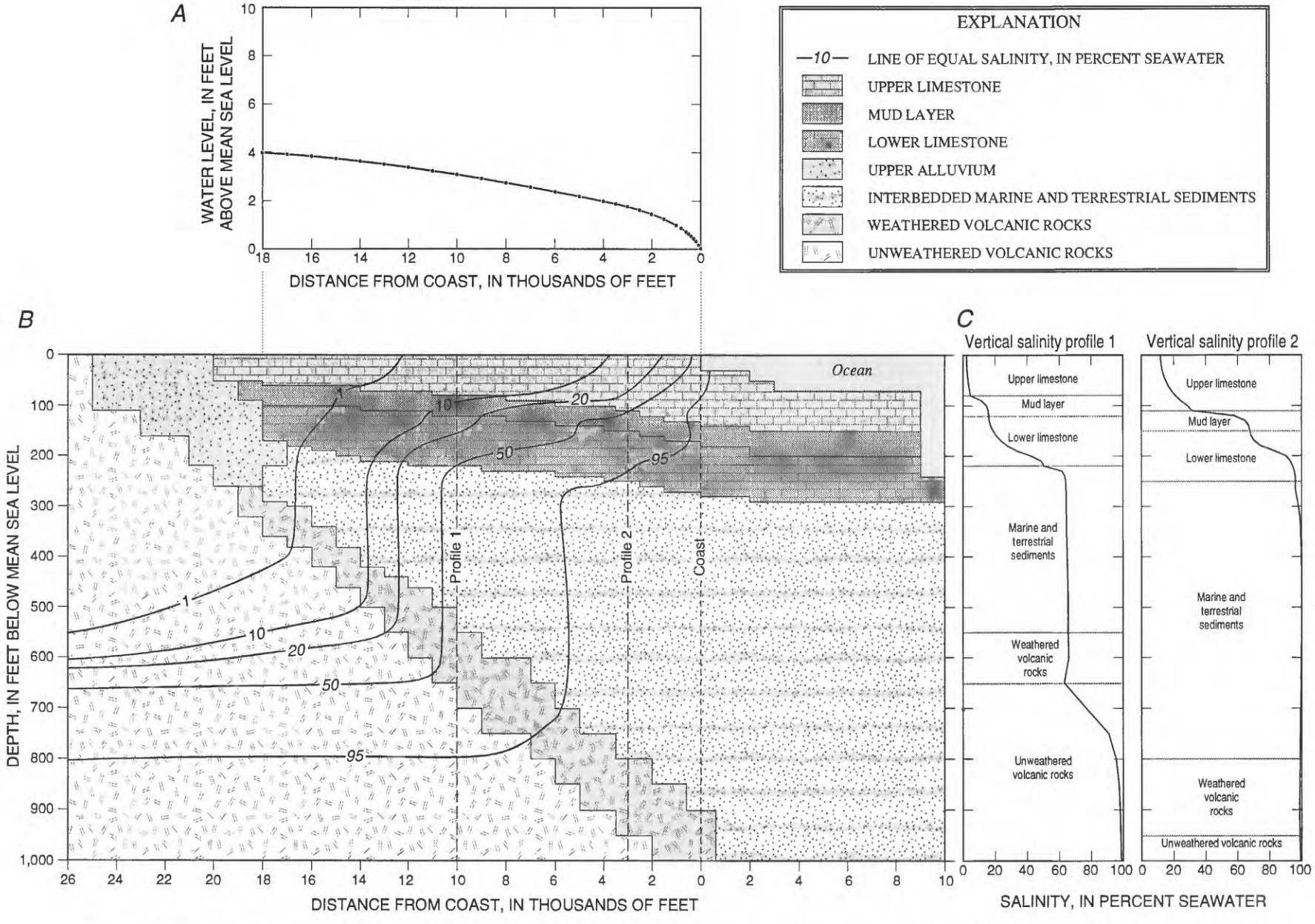

Figure 10. Model-calculated results for scenario 1; *A*, water levels at the top of the upper limestone layer; *B*, lines of equal salinity in the volcanic rocks and caprock; *C*, vertical salinity profiles at distances of 10,000 feet (profile 1) and 3,000 feet (profile 2) inland from the coast.

Water levels in the upper limestone layer.--Model-calculated water levels at the top of the upper limestone layer are shown in figure 10*A*. The water levels represent the height of the water column, measured relative to mean sea level, which would be observed in piezometers located at the top of the upper limestone. Model-calculated water levels at the top of the upper limestone layer vary from 0 ft at the coast to about 4.0 ft above mean sea level near the inland margin of the upper limestone layer, at a distance of 18,000 ft from the coast. These water levels correspond to an average hydraulic gradient of about 1.2 ft/mi.

Simulated freshwater-saltwater flow system in the caprock.--The two main sources of freshwater to the caprock are subsurface inflow from the volcanic rocks and recharge from infiltration of rainfall. The main sources of saltwater to the caprock are direct inflow from the ocean and upward flow from the volcanic rocks.

Results of scenario 1 confirm the general ground-water flow pattern that would be expected in the layered sedimentary ground-water system in the Ewa caprock. The model-calculated directions of ground-water flow are shown in figure 11. Within the caprock, ground-water flow is predominantly vertical in low permeability zones, such as the weathered volcanic rocks, marine and terrestrial sediments, and the mud layer, and predominantly horizontal in the high permeability upper and lower limestone layers. This is consistent with the general flow patterns in a layered freshwater-saltwater flow system described by Rumer and Shiau (1968).

Salinity distribution.--The model-calculated salinity distribution, in terms of percentage of seawater salinity, is shown in figure 10*B* as lines of equal salinity. Lines of equal salinity in the volcanic rocks are predominantly horizontal and indicate an increase of salinity with depth. (Note that the vertical scale in figure 10*B* is greatly exaggerated).

Within the lower parts of the caprock, below the lower limestone layer, lines of equal salinity are mainly vertical, and show an increase in salinity in the seaward direction. The salinity distribution within the lower limestone layer is influenced by mixing between seaward flowing fresh or mixed water overlying landward flowing saltwater. Within the upper limestone layer, the salinity distribution is influenced by mixing among seaward flowing freshwater, landward flowing saltwater, and upward flowing mixed water from the mud layer.

Vertical salinity profiles at distances of 10,000 and 3,000 ft inland from the coast are shown in figure 10C. In general, salinity increases with depth in the caprock .

Effects of Overall Caprock Permeability - Scenarios 2 and 3

In the modeled section, the bulk of the caprock is formed by the upper alluvium, marine and terrestrial sediments, and weathered volcanic rocks zones. In scenario 1, these three zones were assigned isotropic hydraulic conductivities of 0.1 ft/d to correspond to the approximate overall hydraulic conductivity of the caprock estimated by Souza and Voss (1987). The isotropic hydraulic conductivities of these three zones were increased to 1.0 ft/d (scenario 2) and decreased to 0.01 ft/d (scenario 3). The hydraulic conductivity for all other zones remained the same as in scenario 1. Scenarios 2 and 3 are representative of the effects of the overall caprock hydraulic conductivity on: (1) amount of ground-water inflow from the volcanic rocks, (2) water levels in the upper limestone, and (3) salinity distribution within the caprock. Model-calculated water levels and salinity distributions for scenarios 2 and 3 are shown in figures 12 and 13, respectively.

Inflow from volcanic rocks.--Because of the inland boundary condition used, the model-calculated inflow of ground water from the volcanic rocks is directly related to the overall hydraulic conductivity of the caprock; that is, as the overall hydraulic conductivity of the caprock is increased, the model-calculated inflow from the volcanic rocks increases (table 4). The model-calculated inflow from the volcanic rocks for scenarios 1, 2, and 3 ranged from 0.2 Mgal/d per mile of cross-sectional width to 5.3 Mgal/d per mile. These inflow rates bracket the range of previous estimates (George A.L. Yuen and Associates, Inc. 1989; Camp Dresser and McKee, 1994).

Water levels in the upper limestone layer.--Model-calculated water levels in the upper limestone layer vary with the amount of inflow from the volcanic rocks (table 4). For scenario 1, water levels in the upper limestone layer range from 0 ft at the coast to 4.0 ft near the inland margin of the upper limestone, at a distance of 18,000 ft from the coast; this results in an average hydraulic gradient of 1.2 ft/mi. For scenario 2, water levels range from 0 ft at the coast to 7.2 ft near the inland margin of the upper limestone (fig. 12*A*), which

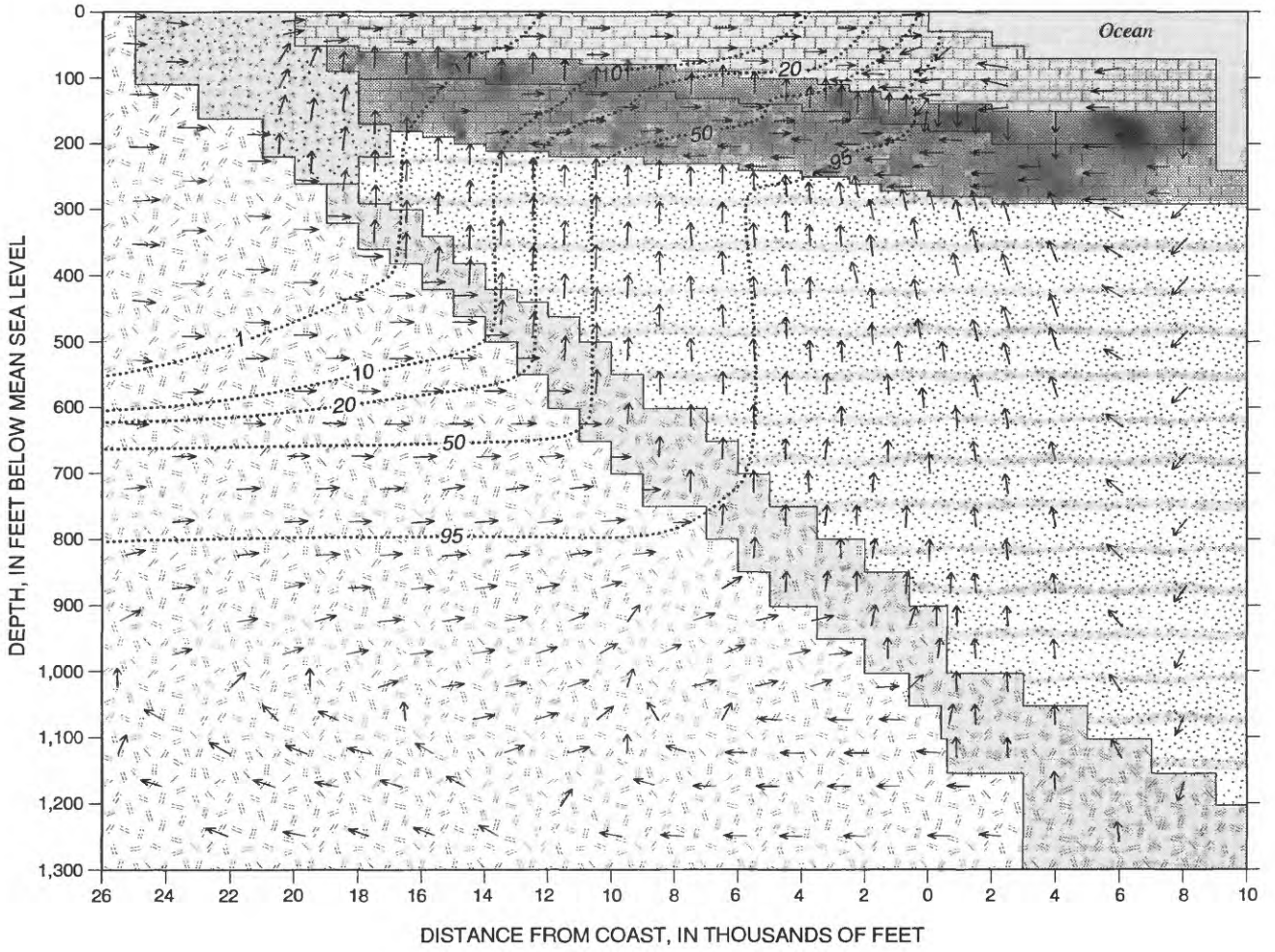

EXPLANATION

- ← DIRECTION OF MODEL-CALCULATED GROUND-WATER FLOW--Orientation of arrows indicate true direction of flow without vertical exaggeration
- ····10···· LINE OF EQUAL SALINITY, IN PERCENT SEAWATER
- UPPER LIMESTONE
- MUD LAYER
- LOWER LIMESTONE
- UPPER ALLUVIUM
- INTERBEDDED MARINE AND TERRESTRIAL SEDIMENTS
- WEATHERED VOLCANIC ROCKS
- UNWEATHERED VOLCANIC ROCKS

Figure 11. Model-calculated ground-water flow directions in the volcanic rocks and caprock for scenario 1.

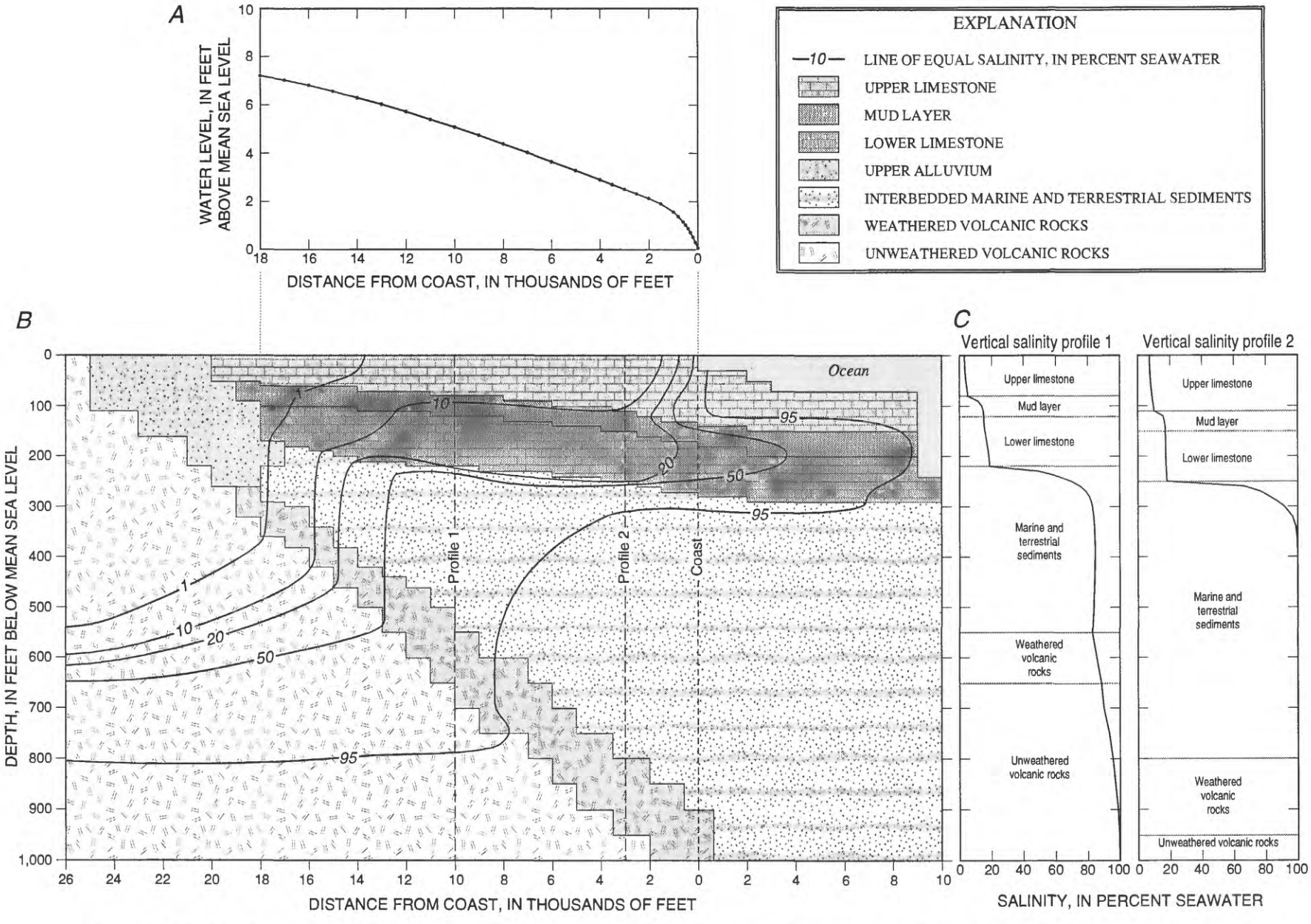

Figure 12. Model-calculated results for scenario 2; *A*, water levels at the top of the upper limestone layer; *B*, lines of equal salinity in the volcanic rocks and caprock; *C*, vertical salinity profiles at distances of 10,000 feet (profile 1) and 3,000 feet (profile 2) inland from the coast.

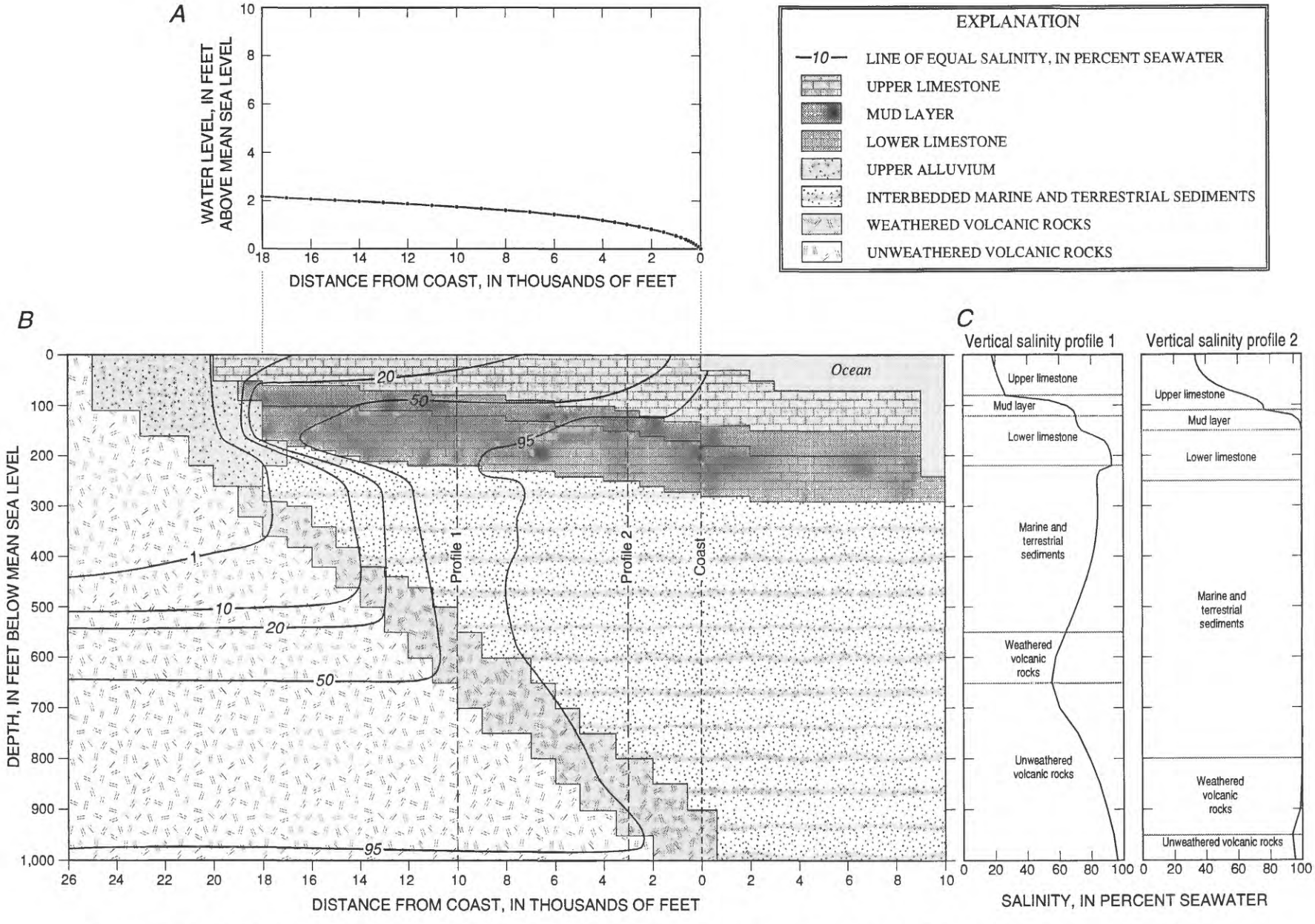

Figure 13. Model-calculated results for scenario 3; *A*, water levels at the top of the upper limestone layer; *B*, lines of equal salinity in the volcanic rocks and caprock; *C*, vertical salinity profiles at distances of 10,000 feet (profile 1) and 3,000 feet (profile 2) inland from the coast.

results in an average hydraulic gradient of 2.1 ft per mile. For scenario 3, water levels range from 0 ft at the coast to 2.2 ft near the inland margin of the upper limestone (fig. 13*A*), which results in an average hydraulic gradient of 0.6 ft per mile.

Salinity distribution.--In scenarios 1 through 3, lines of equal salinity are nearly horizontal in the volcanic rocks, and become roughly vertical in the lower parts of the caprock (figs. 10*B*, 12*B*, and 13*B*). Within the volcanic rocks and lower caprock, lines of equal salinity are generally parallel to the regional ground-water flow direction. Within the upper limestone, mud, and lower limestone layers, salinity is highest in scenario 3 which has the smallest inflow from the volcanic rocks.

Vertical salinity profiles for scenarios 2 and 3 are shown in figures 12C and 13C, respectively. Within the upper limestone layer, the vertical salinity profiles for scenario 2 indicate a uniform concentration with depth at distances of 3,000 and 10,000 ft inland from the coast (fig. 12C). In contrast, in scenario 3, a transition zone develops in the upper limestone layer at a distance of 3,000 ft from the coast (fig. 13C).

Effects of Mud Layer Permeability - Scenario 4

The mud unit separating the upper and lower limestone units is areally extensive in the caprock and is considered a significant hydrogeologic unit. The mud unit has been treated as a confining unit by various investigators. In scenario 1, the layer representing the mud unit was assigned an isotropic hydraulic conductivity of 0.1 ft/d to conform with the overall estimate for the caprock hydraulic conductivity. In scenario 4, the isotropic hydraulic conductivity of the mud layer was reduced from 0.1 ft/d (scenario 1) to 0.001 ft/d. The effects of this reduction in hydraulic conductivity on inflow, water levels, and salinity are described below. Model-calculated water level and salinity distributions for scenario 4 are shown in figure 14.

Inflow from volcanic rocks.--Reducing the hydraulic conductivity of the mud layer results in a reduction of simulated inflow from the volcanic rocks from 1.6 Mgal/d per mile of cross-sectional width to 1.2 Mgal/d per mile. For the modeled boundary conditions, this reduction in inflow is expected because the overall permeability of the caprock is reduced as the hydraulic conductivity of the mud layer is reduced.

Flow across the mud layer.--Reducing the hydraulic conductivity of the mud layer by two orders of magnitude causes a significant reduction in the ground water flow through the mud layer. The model-calculated, fresh-water component of upward flow through the mud layer is 1.2 Mgal/d per mile of cross-sectional width for scenario 1 and 0.09 Mgal/d per mile for scenario 4.

Water levels in the upper limestone layer.--Within the upper limestone layer, model-calculated water levels for scenario 4 increase from 0 ft at the coast to 2.4 ft near the inland margin of the upper limestone (fig. 14*A*). These water levels correspond to an average hydraulic gradient of about 0.7 ft/mi. This is less than the average hydraulic gradient of about 1.2 ft/mi for scenario 1 because the ground-water flow rate in the upper limestone layer for scenario 4 is less than the flow rate for scenario 1, mainly as a result of the reduction of upward flow through the mud layer from the lower limestone layer.

Salinity distribution.--Lines of equal salinity for scenarios 1 and 4 are presented in figures 10*B* and 14*B*, respectively. The effects of the reduced hydraulic conductivity of the mud layer on the distribution of salinity is most pronounced in the upper and lower limestone layers. In general, ground water in both of these layers is fresher in scenario 4 than in scenario 1. Ground water in the lower limestone layer is fresher because in scenario 4 less ground water flows upward through the mud layer and a greater component of freshwater remains within the lower limestone layer. Ground water in the upper limestone layer is fresher because in scenario 4 a smaller component of saltwater flows upward through the mud layer. Within a few thousand feet inland from the coast, however, model-calculated salinity in the upper limestone is greater in scenario 4 than scenario 1. This is a result of increased saltwater intrusion near the coast when the discharge of fresh ground water from the upper limestone is reduced.

Continuity of the mud layer.--It is not expected that the areally extensive mud unit in the Ewa caprock is perfectly uniform and continuous in nature. In areas where the mud unit is thin or absent, flow between the upper and lower limestone units will be enhanced. Thus, the continuity of the mud unit may have a significant effect on the local salinity distribution in the upper limestone unit. To test the importance of

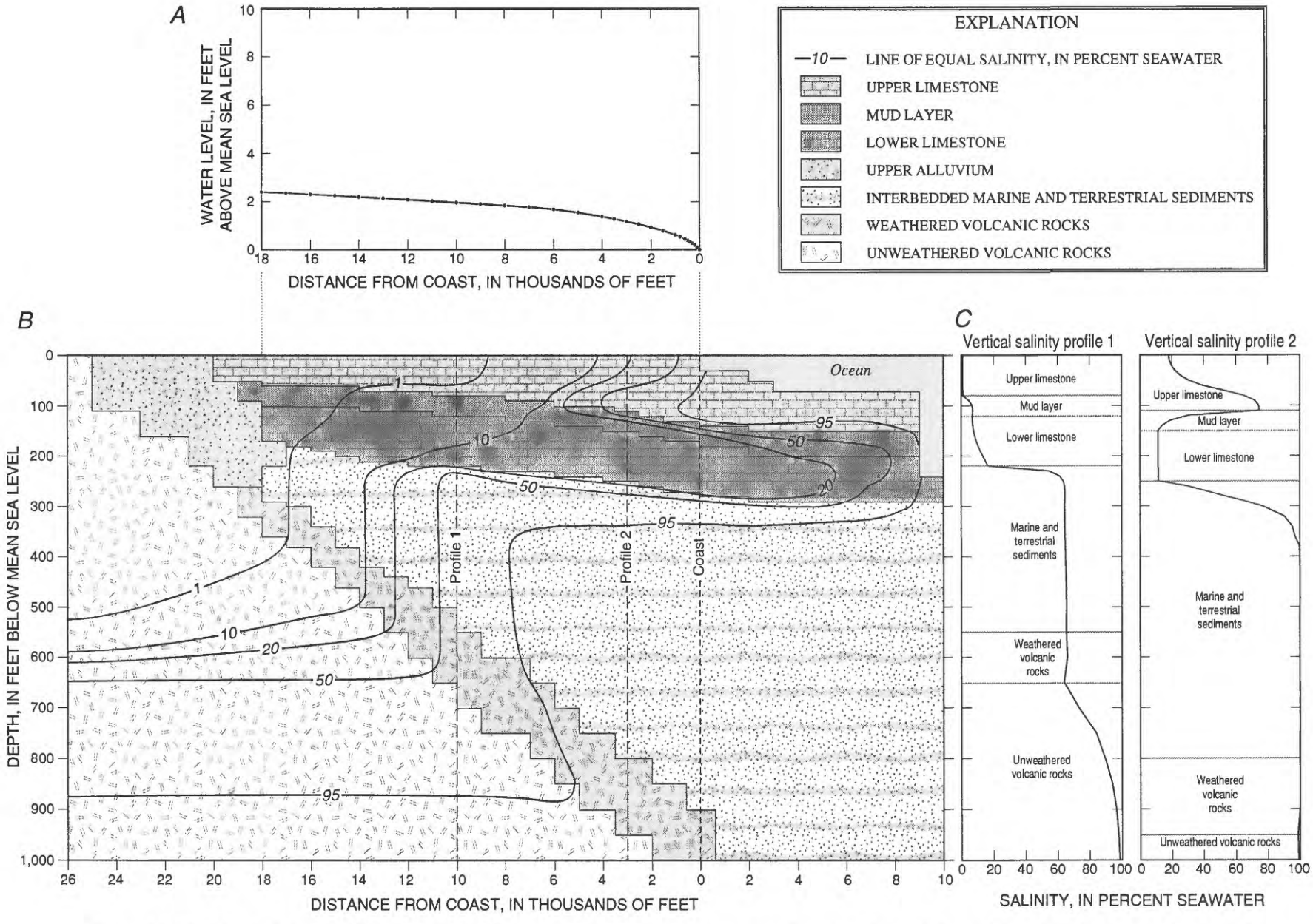

Figure 14. Model-calculated results for scenario 4; *A*, water levels at the top of the upper limestone layer; *B*, lines of equal salinity in the volcanic rocks and caprock; *C*, vertical salinity profiles at distances of 10,000 feet (profile 1) and 3,000 feet (profile 2) inland from the coast.

the mud unit continuity, scenario 4 was modified slightly by creating a 1,000-ft long zone in the modeled mud layer that represents either a thinner or more permeable zone. The zone was simulated by increasing the hydraulic conductivity of the mud layer from 0.001 to 1.0 ft/d between distances of 6,000 and 7,000 ft inland from the coast. This zone represents about 5 percent of the total modeled length of the mud layer. In this simulation, the model-calculated freshwater component of upward flow through the mud layer increased significantly, from less than 0.1 Mgal/d per mile of cross-sectional width in scenario 4 to more than 1 Mgal/d per mile with the introduction of the permeable zone. For this test of mud layer continuity, the upward flow of water through the permeable mud layer zone also increased the salinity in the upper limestone layer. The effects on salinity in the upper limestone layer are likely dependent on the location of the discontinuity because there can be flow of freshwater, mixed water, and saltwater through the mud at various distances from the coastline.

Effects of Layered Heterogeneity in the Upper Limestone Layer- Scenarios 5 and 6

The limestone units of the Ewa caprock are heterogeneous in nature. Dissolution of the rock leads to zones of higher permeability, whereas the presence of muds leads to zones of lower permeability within the limestone units. Because it is common for these zones to be closely related to stratigraphy, their presence may result in a distinct pattern of layered heterogeneity. In addition, Camp Dresser and McKee (1994) suggest that there may be an extensive zone of very high permeability within the upper limestone unit between 50 and 80 ft below sea level at the coast.

Scenarios 5 and 6 are representative of the effects of layered heterogeneity within the upper limestone on the ground-water flow system in the caprock. In both scenarios 5 and 6, the upper limestone was divided into two layers with large contrasts in hydraulic conductivities (figs. 15 and 16). Compared with scenario 1, in scenario 5 a large horizontal hydraulic conductivity (30,000 ft/d) was assigned to the top 20 ft of the upper limestone and the same horizontal hydraulic conductivity (3,000 ft/d) was assigned to the lower part of the upper limestone. In scenario 6, a small horizontal hydraulic conductivity (300 ft/d) was assigned to the top 50 ft of the upper limestone and a large horizontal hydraulic conductivity (30,000 ft/d) was assigned to the lower part of the upper limestone. Since the actual hydraulic conductivity distribution in the upper limestone is unknown, these hydraulic conductivity distributions were selected to represent two vastly different lithologic structures for the upper limestone layer. The effects of layered heterogeneity of the upper limestone layer for these hydraulic conductivity distributions can be seen by comparing figures 15 and 16 with figure 10.

Inflow from volcanic rocks.--In scenarios 5 and 6, the model-calculated inflows from the volcanic rocks are 1.7 and 1.6 Mgal/d per mile of cross-sectional width, respectively. These inflows are similar to the inflow of 1.6 Mgal/d per mile from scenario 1. Model-calculated inflow rates from the volcanic rocks, however, are actually slightly higher in scenarios 5 and 6 relative to scenario 1 because an increase in hydraulic conductivity in the upper limestone layer results in a slightly higher overall hydraulic conductivity of the caprock. This increase in hydraulic conductivity of the upper limestone layer also results in lower water levels in the upper limestone and increases the hydraulic gradient between the volcanic rocks and the caprock.

Water levels in the upper limestone layer.--For scenario 5, model-calculated water levels along the top of the upper limestone layer vary from 0 ft at the coast to 1.7 ft near the inland margin of the upper limestone (fig. 15*A*), corresponding to an average hydraulic gradient of about 0.5 ft per mile. For scenario 6, water levels at the top of the upper limestone layer vary from 0 ft at the coast to 2.8 ft near the inland margin of the upper limestone (fig. 16*A*), which results in an average hydraulic gradient of 0.82 ft per mile. The model-calculated hydraulic gradient for scenario 5 is smaller than that of scenario 6 because the top of the upper limestone layer was assigned a higher hydraulic conductivity in scenario 5. Both scenarios 5 and 6 produced smaller average hydraulic gradients at the top of the upper limestone layer than scenario 1.

Salinity distribution.--Lines of equal salinity within the caprock for scenarios 5 and 6 are shown in figures 15*B* and 16*B*, respectively. Within the upper limestone, mud, and lower limestone layers, scenarios 5 and 6 produced higher salinities than scenario 1. This is also apparent by comparing the vertical salinity profiles shown in figures 15C and 16C with the salinity profiles for scenario 1 (fig. 10C). The higher salinity associated with scenarios 5 and 6 is caused by increased saltwater intrusion associated with lower water levels in the upper layers.

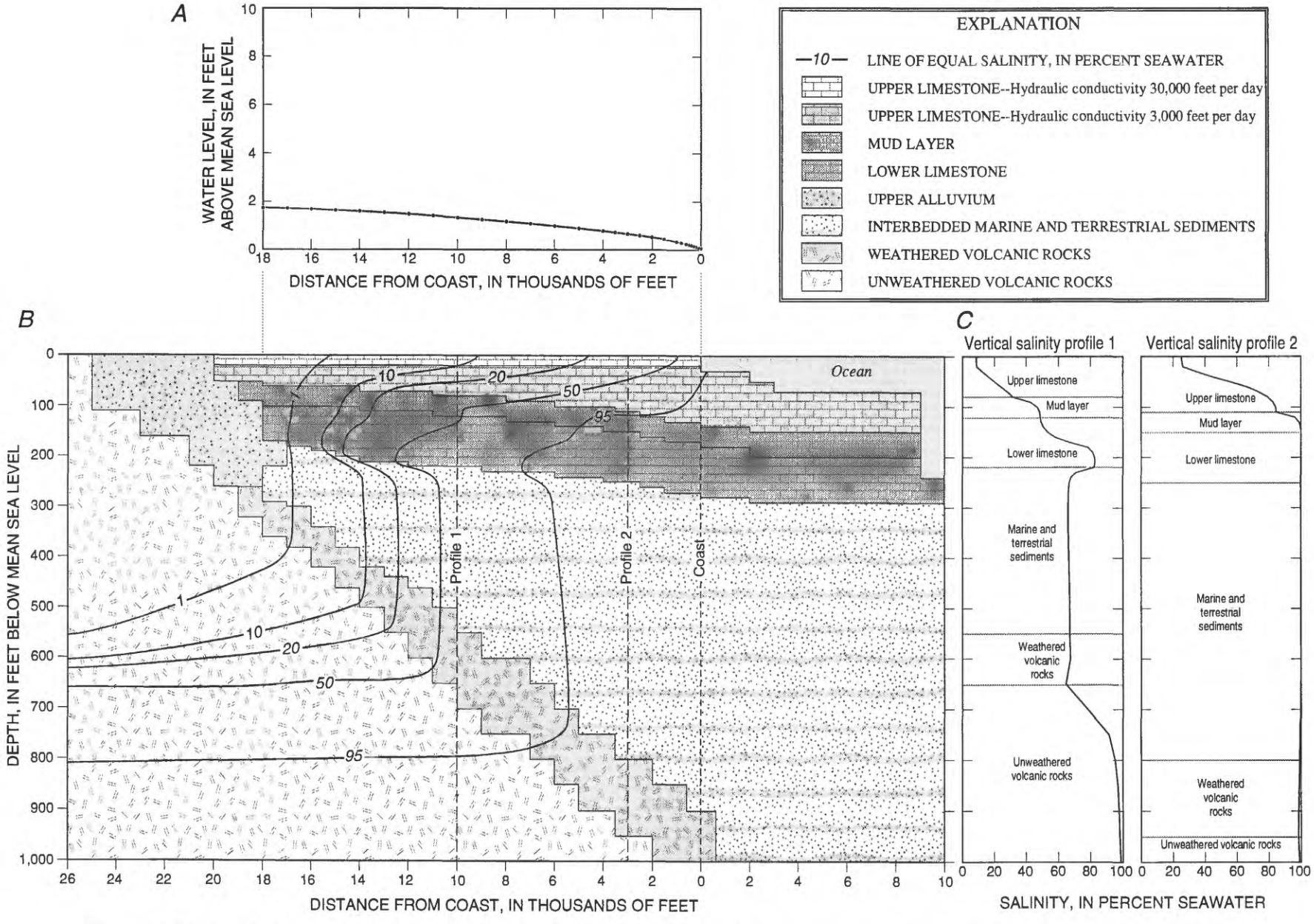

Figure 15. Model-calculated results for scenario 5; *A*, water levels at the top of the upper limestone layer; *B*, lines of equal salinity in the volcanic rocks and caprock; *C*, vertical salinity profiles at distances of 10,000 feet (profile 1) and 3,000 feet (profile 2) inland from the coast.

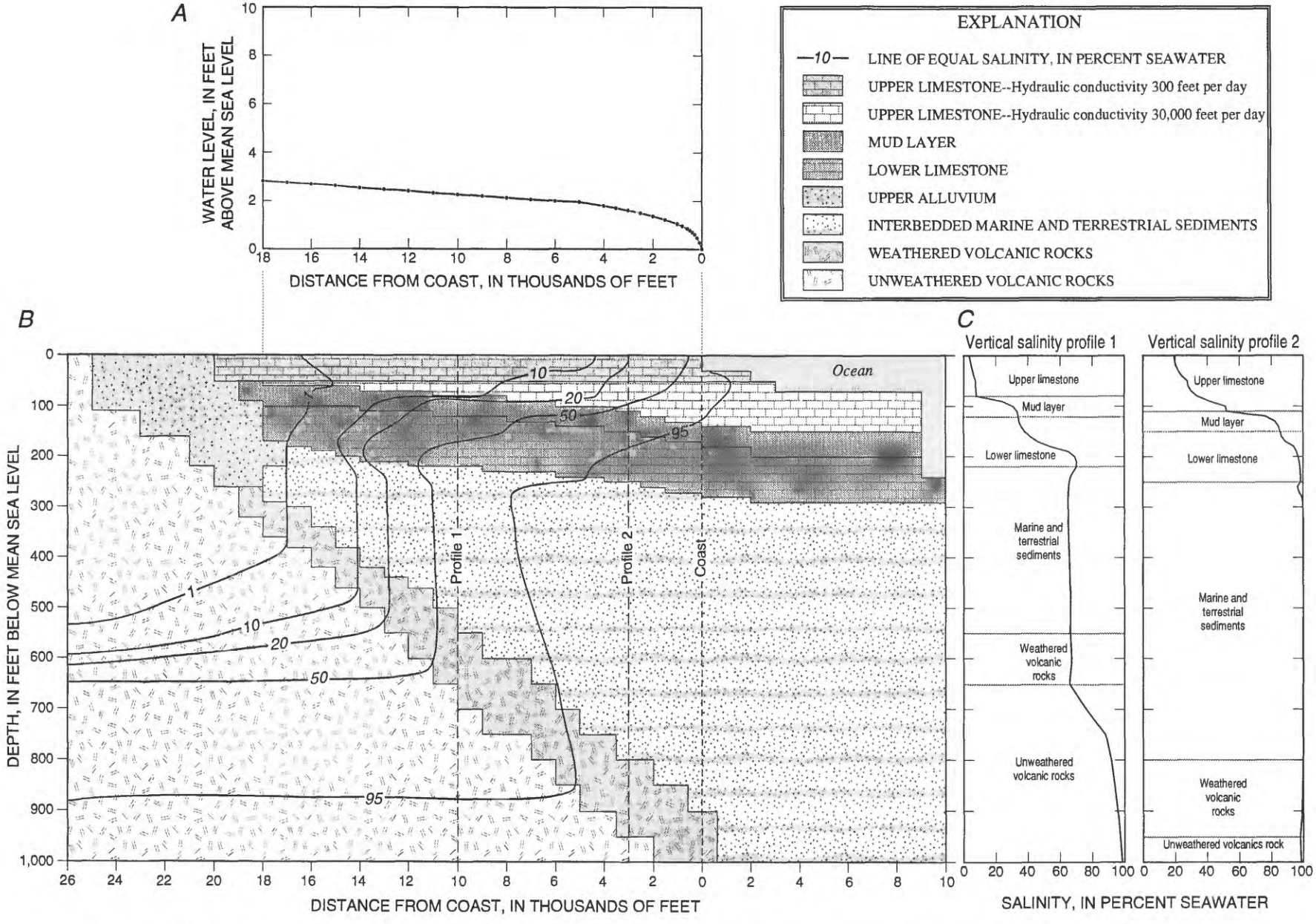

Figure 16. Model-calculated results for scenario 6; *A*, water levels at the top of the upper limestone layer; *B*, lines of equal salinity in the volcanic rocks and caprock; *C*, vertical salinity profiles at distances of 10,000 feet (profile 1) and 3,000 feet (profile 2) inland from the coast.

These scenarios demonstrate the significant effects that lithologic structure have on the vertical salinity profile in the upper limestone. In scenario 5, the upper part of the upper limestone was assigned a greater hydraulic conductivity than the lower part. The model-calculated vertical salinity profiles for scenario 5 (fig. 15C) show a distinct increase in salinity at the base of the upper sublayer of the upper limestone. In scenario 6, the lower part of the upper limestone was assigned a greater hydraulic conductivity than the upper part. The vertical salinity profiles for scenario 6 (fig. 16C) indicate an increase of salinity with depth. However, the rate of salinity increase with depth decreases abruptly at the contact between the upper and lower sublayers.

Effects of Ending Irrigation Recharge - Scenario 7

For a furrow-irrigated sugarcane land use, average annual ground-water recharge to the Ewa caprock is estimated to be about 83.8 in. (Giambelluca, 1986). In scenario 7, 75 percent of the land area over the caprock was assumed to be furrow-irrigated sugarcane, which resulted in total recharge of 8.5 Mgal/d per mile of cross-section width. In this scenario, pumping in the caprock was assumed to be 4 Mgal/d. The effects of eliminating the irrigation return flow component can be seen by comparing water levels and salinity distributions from scenarios 7 and 1. For both scenarios, a 17-ft head at the inland boundary of the volcanic rocks was maintained.

Inflow from volcanic rocks.--For scenarios 7 and 1, model-calculated inflows from the volcanic rocks are 1.3 and 1.6 Mgal/d per mile of cross-sectional width, respectively. The increase in model-calculated inflow following cessation of furrow irrigation (scenario 7 to scenario 1 progression) is because water levels in the upper limestone layer are lower in scenario 1 than in scenario 7. The lower water levels result in an increased hydraulic gradient between the volcanic rocks and the upper limestone layer in scenario 1 and a greater inflow from the volcanic rocks. The model-calculated increase of inflow from the volcanic rocks of about 0.3 Mgal/d per mile, however, is small compared to the reduction in recharge from 8.5 Mgal/d per mile in scenario 7 to 0.45 Mgal/d per mile in scenario 1.

Water levels in the upper limestone layer.--The model-calculated water levels in the upper limestone layer for scenario 7 vary from 0 ft at the coast to 8.1 ft near the inland margin of the upper limestone (fig. 17*A*). When the irrigation return flow and pumpage are removed (scenario 1), the model-calculated water levels in the upper limestone vary from 0 ft at the coast to 4.0 ft near the inland extent of the upper limestone. The reduced hydraulic gradient in the upper limestone layer caused by elimination of the irrigation return flow is an expected consequence of the reduction of ground-water flow through the upper limestone.

It should be noted that the model-calculated water levels for scenarios 1 and 7 are higher than observed water levels in the upper limestone unit. This suggests that either inflow from the volcanic aquifer is overestimated or the hydraulic conductivity of the upper limestone unit is underestimated in these two scenarios. In addition, the actual geometry of the upper limestone layer may not be accurately represented in the model.

Salinity distribution.--The model-calculated salinity distributions for scenarios 1 and 7 are presented in figures 10*B* and 17*B*, respectively. The salinity distributions differ between scenarios 1 and 7, primarily above the base of the lower limestone layer. In scenario 7, irrigation return flow freshens the ground water in the upper limestone layer. In addition, downward flow of fresh ground water from the upper limestone through the mud layer and into the lower limestone layer results in a freshening of ground water in both the mud and the lower limestone layers. Vertical salinity profiles at distances of 10,000 and 3,000 ft inland from the coast are shown for scenarios 1 and 7 in figures 10*C* and 17*C*, respectively. These profiles indicate that within the upper limestone, mud, and lower limestone layers, ground water has lower salinity in scenario 7 because of increased recharge from irrigation return flow. Below the lower limestone layer, the effects of the furrow irrigation on ground-water quality are less pronounced. For both scenarios, salinity increases with depth below the lower limestone layer.

Effects of Excavating an Ocean Marina - Scenarios 8 through 10

The effects of excavating an ocean marina were evaluated as part of this study. The marina was assumed to be 20 ft deep and extend 1,500 ft inland from the

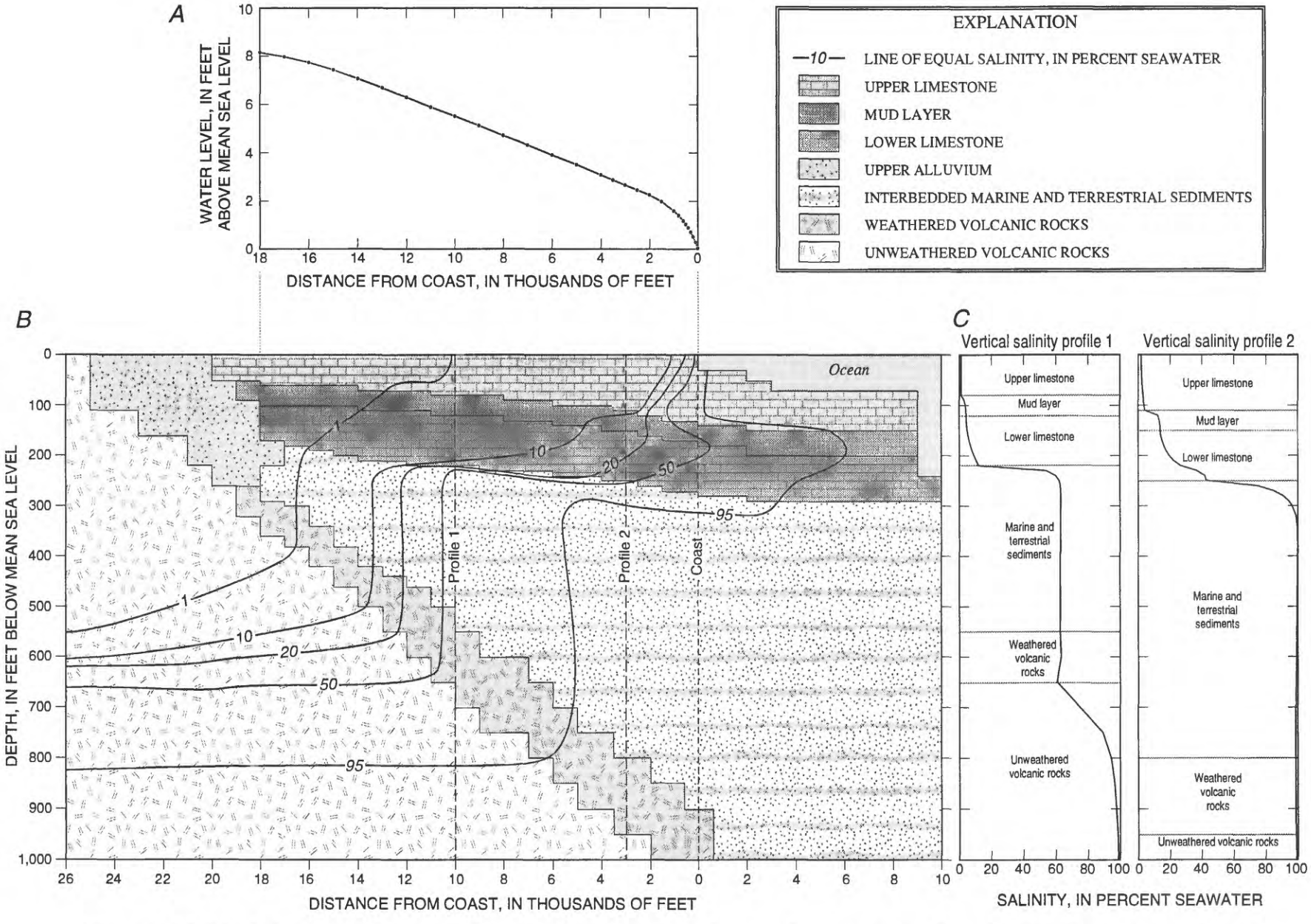

Figure 17. Model-calculated results for scenario 7; *A*, water levels at the top of the upper limestone layer; *B*, lines of equal salinity in the volcanic rocks and caprock; *C*, vertical salinity profiles at distances of 10,000 feet (profile 1) and 3,000 feet (profile 2) inland from the coast.

coast (figs. 18, 19, and 20) The excavated part of the upper limestone was simulated in the model with the same hydrostatic saltwater boundary condition used for the ocean in previous simulations. The marina-excavation scenarios 8 through 10 used the hydraulic conductivity distributions of scenarios 3 through 5, respectively. These scenarios represent a range of reasonable hydraulic conductivity values for the caprock layers. Scenarios 3 through 5 also produced model-calculated water levels in the upper limestone layer that were within the range of observed water levels. In addition, the scenarios represented a range of inflow values from the volcanic rocks, 0.2 to 1.7 Mgal/d per mile.

Inflow from the volcanic rocks.--In scenarios 8 through 10, excavation of a marina lowers water levels in the upper limestone layer and thus induces a small increase in flow from the volcanic aquifer to the caprock. For the scenarios tested, model-calculated inflow rates from the volcanic rocks changed by less than 0.01 Mgal/d per mile of cross-sectional width with the introduction of the marina excavation.

Water levels in the upper limestone layer.--Model-calculated water levels in the upper limestone layer decline in response to the simulated marina excavation, which causes a landward shift in the upper part of the discharge zone in the upper limestone. The water-level declines are greatest near the marina excavation (about 0.4 to 0.8 ft) and are about 0.1 to 0.2 ft near the inland margin of the upper limestone layer (figs. 18*A*, 19*A*, 20*A*). The water-level declines depend on the hydraulic conductivity of the upper limestone layer. Within 1,000 ft inland from the marina, the greatest decline in water levels was simulated in scenario 9 and the smallest decline in scenario 10.

Salinity distribution.--Model-calculated vertical salinity profiles for scenarios 8 through 10 are shown in figures 18*C*, 19*C*, and 20*C*. Model-calculated lines of equal salinity in the caprock are shown in figures 18*B*, 19*B*, and 20*B*. These figures may be compared with figures 13*B*, 14*B*, and 15*B* to show the changes in salinity induced by the marina excavation. In general, the simulated marina excavation causes an inland shift in the lines of equal salinity. Within the upper limestone layer, the effects are greatest near the marina and lessen with distance inland.

MODEL LIMITATIONS

The cross-sectional model developed for this study was used to evaluate the controls on the ground-water flow system in the Ewa area. The main limitation of this cross-sectional approach is that ground-water is forced to flow within and parallel to the modeled section. There is no lateral discharge from or inflow to the sides of the cross section. Thus, for example, the cross-sectional model cannot account for the possible easterly discharge of ground water to West Loch (fig. 2). The model also cannot simulate the areally varying flow, water levels, and salinity distribution in the direction transverse to the modeled section.

In terms of simulating an ocean marina, the use of a cross-sectional model should provide a conservative estimate of the regional effects of the excavation. A marina occupies a part of the coastline, leaving the non-excavated part of the coastline intact. However, by using a cross-sectional model to simulate the excavation, it is assumed that the marina will occupy the entire coastline. Thus, for a given set of aquifer parameters, the regional effects of an excavation, in terms of water-level declines and salinity changes, should be overestimated by a cross-sectional model.

Because the model presented here is not calibrated, this presents additional limitations on interpretations that can be drawn from the model results. For instance, the actual effects of excavating an ocean marina cannot be predicted with this model. Although results using a plausible range of aquifer parameters indicate that there will be water-level declines and salinity increases in the upper limestone unit caused by excavation of an ocean marina, the magnitude of the water-level and salinity changes cannot be predicted without a properly calibrated model.

CONCEPTUAL MODEL OF THE GROUND-WATER FLOW SYSTEM

On the basis of the cross-sectional model results, a refined conceptual model of the regional ground-water flow system in the Ewa area was developed. The conceptual model of the regional flow system presented below was formulated using a generalized stratigraphic representation of the caprock and presents the general freshwater, saltwater, and mixed-water flow patterns

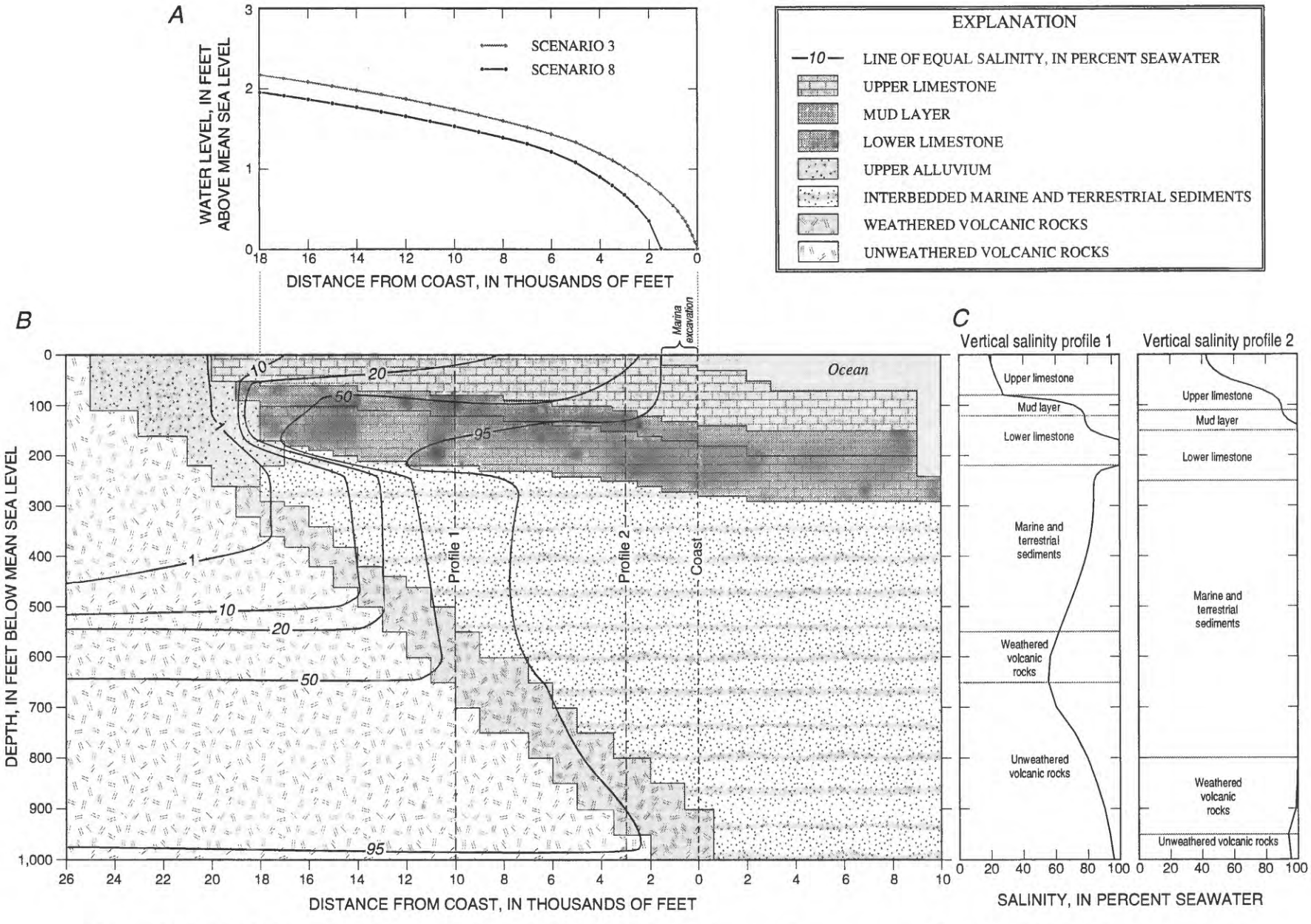

Figure 18. Model-calculated results for scenario 8; *A*, water levels at the top of the upper limestone layer; *B*, lines of equal salinity in the volcanic rocks and caprock; *C*, vertical salinity profiles at distances of 10,000 feet (profile 1) and 3,000 feet (profile 2) inland from the coast.

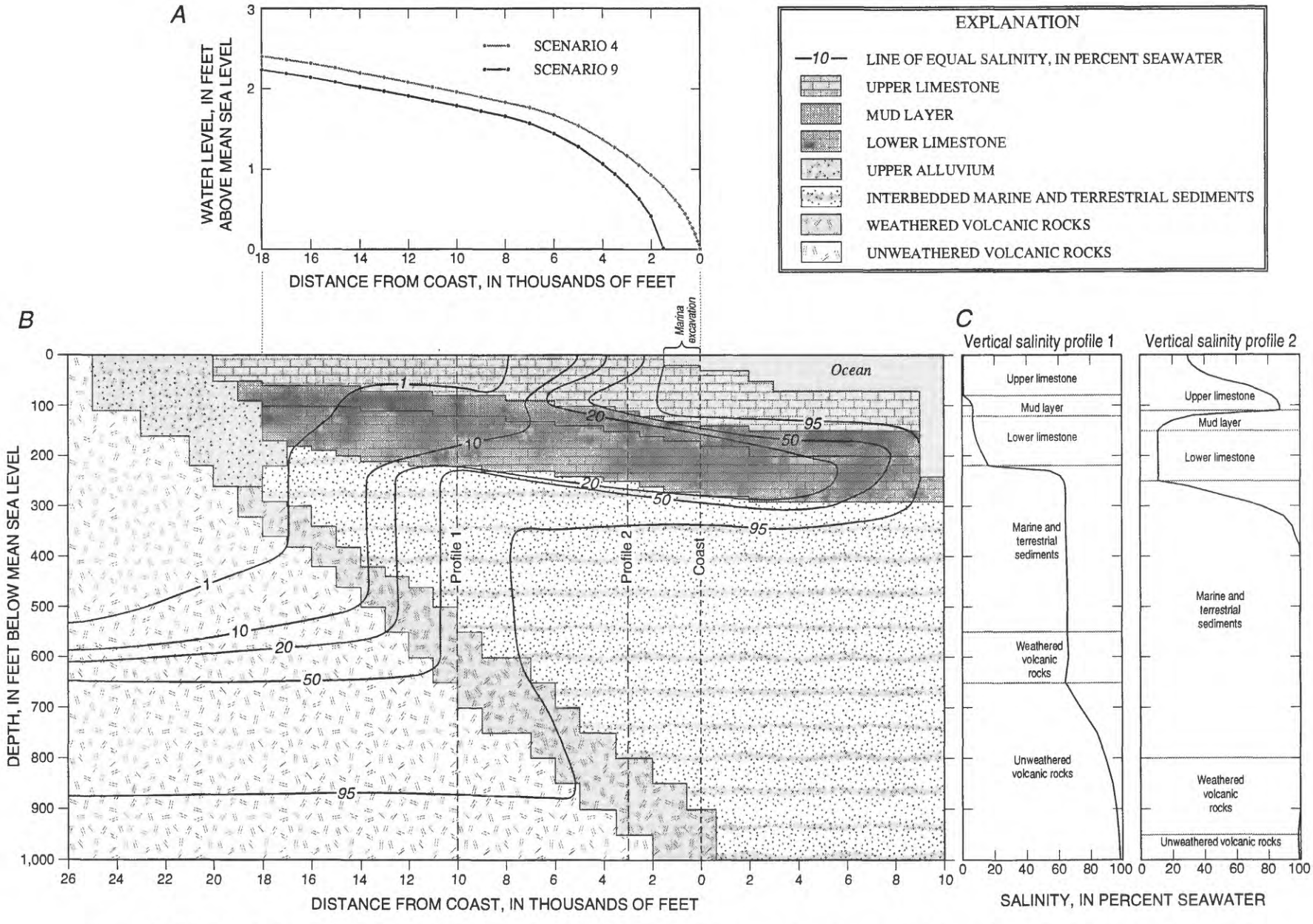

Figure 19. Model-calculated results for scenario 9; *A*, water levels at the top of the upper limestone layer; *B*, lines of equal salinity in the volcanic rocks and caprock; *C*, vertical salinity profiles at distances of 10,000 feet (profile 1) and 3,000 feet (profile 2) inland from the coast.

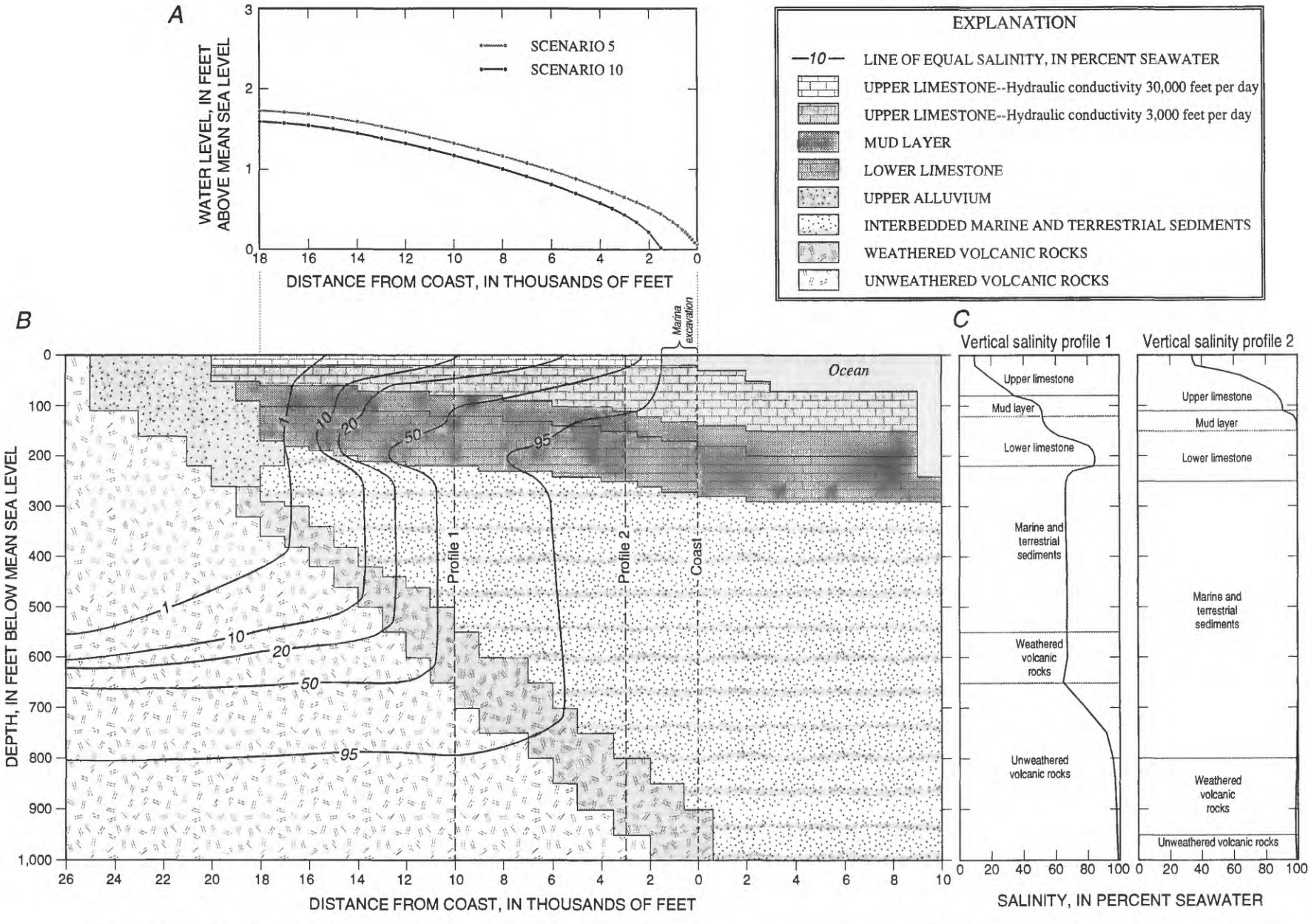

Figure 20. Model-calculated results for scenario 10; *A*, water levels at the top of the upper limestone layer; *B*, lines of equal salinity in the volcanic rocks and caprock; *C*, vertical salinity profiles at distances of 10,000 feet (profile 1) and 3,000 feet (profile 2) inland from the coast.

within the volcanic rocks and caprock. The heterogeneous and complex nature of the caprock stratigraphy make it impossible to fully describe local-scale phenomena within the caprock.

Volcanic rocks.--Within the volcanic aquifers of the Ewa area, the ground-water flow system is composed of a freshwater lens overlying a zone of transition to a saltwater body. Figure 21 shows the generalized fresh and saltwater flow patterns within the volcanic aquifers (Souza and Voss, 1987). The following numbered paragraphs and descriptions correspond to the numbered locations in figure 21.

(1)

The source of freshwater forming the lenses within the volcanic aquifers is ground-water recharge from rainfall and irrigation return flow. In the inland recharge areas, the aquifers are unconfined. Fresh ground water in this area has a predominantly downward flow component.

(2)

Fresh ground water in the volcanic aquifers moves from inland recharge areas toward coastal discharge areas. Between the recharge and discharge areas, flow is predominantly horizontal.

(3)

The volcanic aquifers are confined by the sedimentary caprock that impedes the seaward discharge of fresh ground water from the volcanic aquifers. Near the coast, fresh ground water flows upward in the volcanic aquifers toward the caprock.

(4)

The landward inflow of seawater into the volcanic aquifers is impeded by the sedimentary caprock.

(5)

Saltwater within the volcanic aquifers also is derived from the ocean from deep circulation in the volcanic rocks.

(6)

A saltwater circulation system exists beneath the freshwater lens. Saltwater flows landward in the deeper parts of the aquifers, rises, and then mixes with fresher water. This mixing creates a saltwater-freshwater transition zone.

(7)

The mixed water within the transition zone and freshwater ***(3)*** flow from the volcanic aquifers into the caprock.

Caprock.--The Ewa caprock is composed of numerous sedimentary layers of varying permeabilities. Ground-water movement and salinity distribution in a layered system such as this are controlled by the variation and contrasts in permeability of the layers. The generalized fresh and saltwater flow patterns within the caprock for a generalized stratigraphy are shown in figure 22. The following numbered paragraphs and descriptions correspond to the numbered locations in figure 22.

(1 and 2)

The caprock receives fresh ground water from two sources. The first source is subsurface discharge of freshwater from the underlying volcanic aquifers ***(1)***. The second source is recharge from irrigation return flow and infiltration of rainfall ***(2)***.

(3 and 4)

In general, flow of freshwater within the caprock is predominantly vertical ***(3)*** in the low permeability units, such as the weathered volcanic rocks, alluvium, and mud units, and predominantly horizontal ***(4)*** in the high permeability units, such as the limestone units. The direction of freshwater flow in the low permeability units may be either upward or downward depending on the relative amounts of inflow from ***(1)*** and ***(2)***.

(5)

Water discharging from the volcanic aquifers to the ocean takes the path of least resistance through the caprock. Highly permeable limestone units that crop out beneath the ocean represent preferred flow pathways for freshwater. Thus, a significant amount of ground water may discharge from the volcanic rocks where highly permeable limestone units are in direct contact with volcanic rocks.

(6 and 7)

Within the caprock, preferred vertical flow pathways may exist where the low permeability units are thin or absent ***(6)***, or where highly permeable limestone

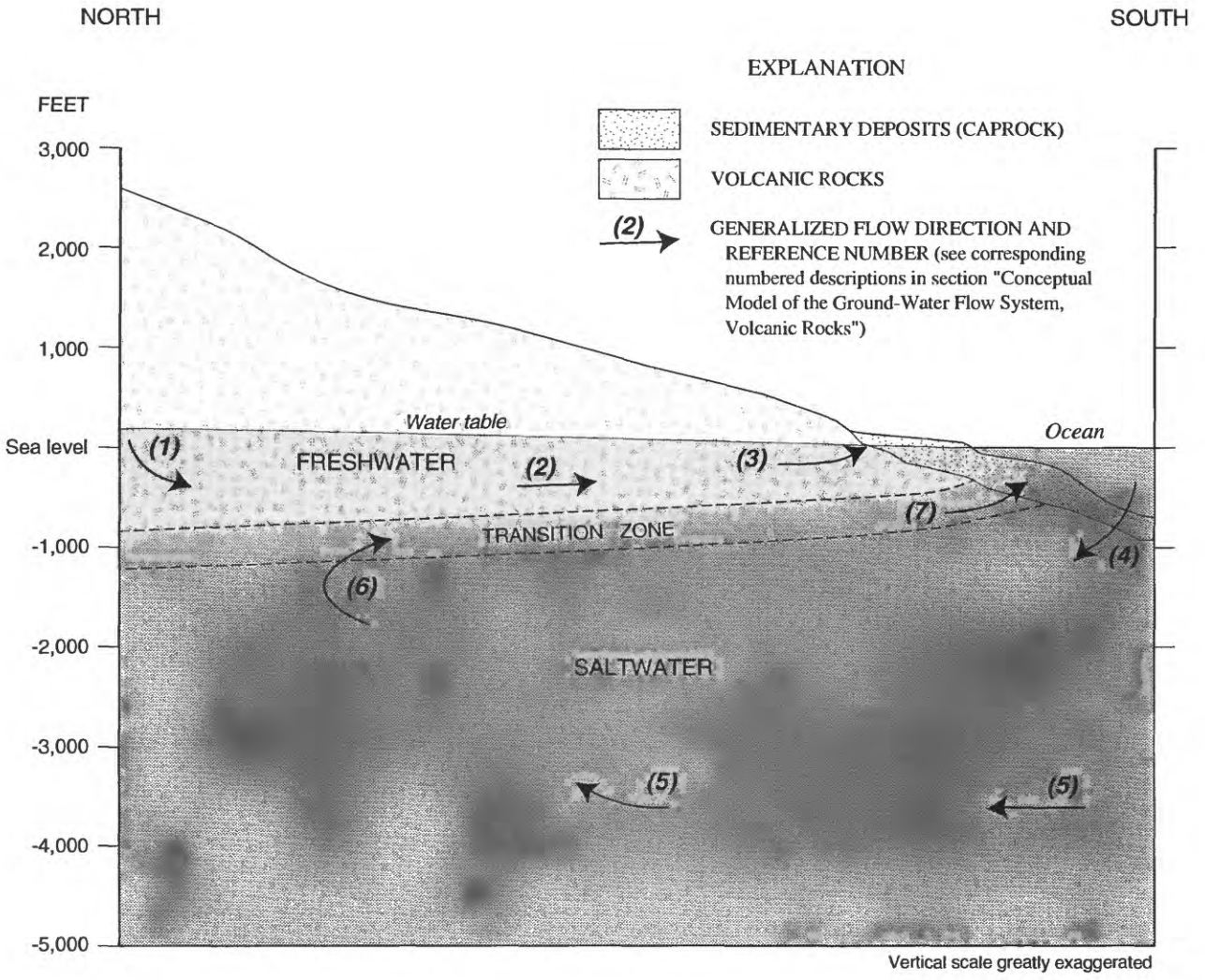

Figure 21. Generalized ground-water flow pattern in the volcanic rocks near Ewa, Oahu, Hawaii (adapted from Souza and Voss, 1987).

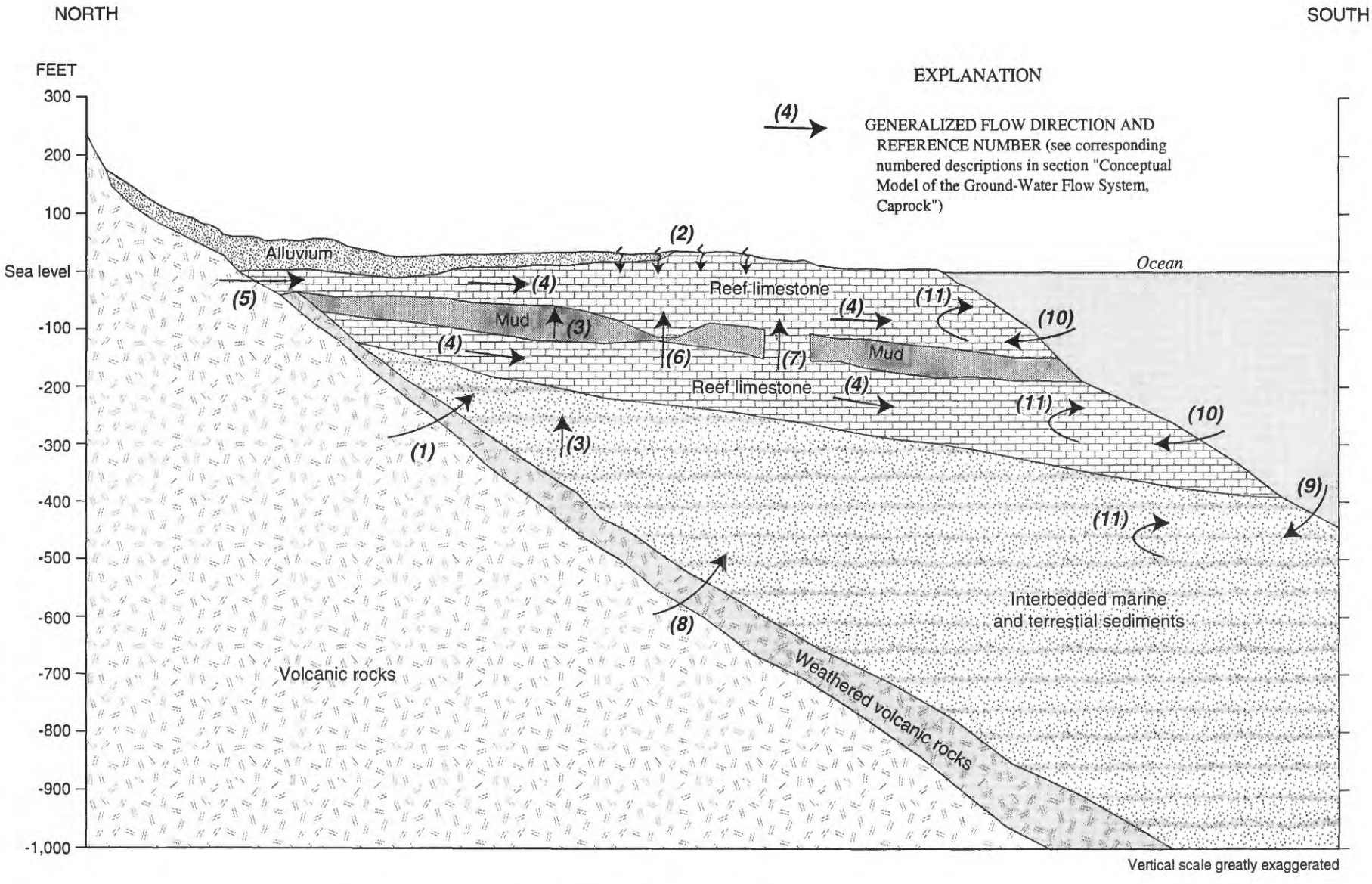

Figure 22. Generalized ground-water flow pattern in the Ewa caprock, Oahu, Hawaii.

structures, formed by patch or pinnacle reefs, exist ***(7)***. The direction of flow through these preferred pathways may be either upward or downward depending on the relative amounts of inflow from ***(1)*** and ***(2)***.

(8 through 10)

There are two primary sources for components of saltwater in the caprock. The first source is the discharge of mixed water from deep in the underlying volcanic aquifers ***(8)***. Mixed water derived from the volcanic aquifers follows discharge paths similar to that described for freshwater in ***(3)*** through ***(7)***. The second source of saltwater to the caprock is inflow of seawater at the ocean bottom ***(9 and 10)***. Highly permeable limestone units exposed at the ocean bottom represent preferred flow pathways for saltwater ***(10)*** as well as for freshwater ***(5)***. Thus, where highly permeable limestone units are in direct contact with the ocean, seawater readily enters the caprock. A third possible source of salts to the caprock is from ***(2)*** but this source is probably small in comparison to ***(8)*** through ***(10)***.

(11)

Landward flowing saltwater derived from the ocean mixes with the seaward flowing fresh and mixed water, creating saltwater circulation cells in most of the individual units of the caprock.

Additional aspects of the conceptual model.--Deep monitor wells, which extend into the freshwater-saltwater transition zone (fig. 4), define the salinity distribution in the volcanic rocks. No comparable deep monitor wells exist in the caprock and, thus, the actual salinity distribution throughout the caprock is unknown except at a few sites in the upper limestone unit. Existing data indicate that the salinity of ground water in the upper limestone unit varies as a function of the quality and quantity of recharge to the upper limestone. In the deeper parts of the caprock, additional high-permeability limestone units below the lower limestone unit may exist and would represent preferred flow pathways for both freshwater and saltwater. These deeper limestone units could have a significant effect on the salinity distribution within the caprock. In addition, the hydraulic conductivity of the weathered volcanic rocks at the base of the caprock could be very low and thus the weathered volcanic rocks could act as a confining unit and would be an important control on salinity in the caprock. However, like the mud unit, there may be preferred pathways where the weathered volcanic rock zones are thin or absent.

Although it is recognized that the hydraulic conductivity distribution in the caprock is an important control on the salinity distribution, it was impractical to exhaustively test all plausible hydraulic conductivity distributions in model simulations. For this study, the upper alluvium, weathered basalt, and marine and terrestrial sediments were assumed to have the same hydraulic conductivity. This parsimonious approach can be refined in the future as more data become available to better characterize the hydraulic conductivity and salinity distributions within these parts of the caprock. The results of model simulations presented in this study identified several major hydrogeologic controls on ground-water flow in the caprock and provide the basis for a generalized conceptual model of the flow system. Details of the actual flow system will vary from the conceptual model presented above. As more data become available, the current understanding of the flow system will be improved and the conceptual model can be further refined.

SUMMARY AND CONCLUSIONS

In the Ewa area, along the southern coast of Oahu, the discharge of fresh ground water from the volcanic aquifers is impeded by the confining sedimentary deposits (caprock) of the coastal plain. A cross-sectional ground-water flow and transport model was used to evaluate hydrogeologic controls on the ground-water flow system in the Ewa caprock. The model was used to examine the effects of variations in hydraulic conductivity and recharge on: (1) water levels in the upper limestone layer, (2) salinity distribution in the caprock, and (3) amount of ground-water flow through the caprock. The model explored a limited number of reasonable hydraulic conductivity distributions through numerical simulation. On the basis of these simulations, several general statements and conclusions can be made:

1. The amount of freshwater flow between the volcanic aquifers and the caprock is controlled by the overall hydraulic conductivity of the caprock. For this study, the model-calculated inflow from the volcanic rocks varied from 0.2 to 5.3 Mgal/d per mile of cross-sectional width. This range of inflow rates brackets the

range of previously estimated inflow rates from the volcanic rocks.

2. The amount of ground-water flow between the volcanic aquifers and the caprock is an important factor controlling water levels and salinity distribution in the caprock; however, the actual amount of flow cannot be determined with cross-sectional modeling using currently available data. Model results can reproduce general conditions in the upper limestone layer within a range of values of ground-water flow tested.

3. Within the caprock, variations in hydraulic conductivity as a result of the caprock stratigraphy are a major control on the amount and direction of ground-water flow, and the distribution of water levels and salinity.

4. The continuity and hydraulic conductivity of the mud layer controls the amount of ground-water flow between the upper limestone layer and the sedimentary layers below the mud. Model results indicate that there can be both upward and downward flow of freshwater and saltwater through the mud layer. Zones of high permeability or small discontinuities in the mud layer may allow significant flow between the upper limestone layer and the sedimentary layers below the mud.

5. Model results show that within the upper limestone layer the water level and salinity distributions are controlled by the: (a) amount of ground-water flow, (b) stratigraphic variations within the upper limestone, and (c) continuity and hydraulic conductivity of the mud layer.

6. The end of agricultural irrigation will result in a reduction of recharge from irrigation return flow. For the conditions simulated, in which pumping from the volcanic aquifers was not considered, model results show that a reduction of recharge will result in increased salinity throughout the caprock with the greatest change in the upper limestone layer. Within the upper limestone layer, model results show a decline in water levels in response to the reduction in low-salinity recharge.

7. Excavation of an ocean marina causes a landward shift in the upper part of the ground-water discharge zone in the upper limestone layer. Model results show that this shift will lower water levels in the upper limestone layer. Results also show that lines of equal salinity will generally shift landward in response to the landward shift of the discharge zone.

8. Results of cross-sectional modeling confirm the general ground-water flow pattern that would be expected in the layered sedimentary Ewa caprock and volcanic rocks. Both freshwater and mixed freshwater-saltwater flow from the volcanic aquifers into the caprock. This inflow from the volcanic aquifers further mixes with freshwater and saltwater in the caprock before discharging into the ocean. Ground-water flow within the Ewa caprock is: (1) predominantly upward in the low-permeability sedimentary units, and (2) predominantly horizontal in the high-permeability sedimentary units. The layered stratigraphy of the caprock results in a complex freshwater-saltwater flow system throughout the caprock.

9. A cross-sectional ground-water flow and transport model is a useful tool to evaluate hydrogeologic controls on the caprock flow system and to develop a conceptual model of the regional flow system. However, additional data are needed to calibrate any numerical model that includes simulation of the caprock.

10. Additional data are needed to improve the conceptual model of the flow system. Specific data and information needs include: (a) water-level and salinity data in the lower sedimentary units, (b) hydraulic conductivity of the mud unit, and (c) amount of ground-water flow from the volcanic aquifers to caprock.

REFERENCES CITED

Bauer, Glenn, 1996, Reevaluation of the ground-water resources and sustainable yield of the Ewa caprock aquifer, prefinal draft report: State of Hawaii, Department of Land and Natural Resources, Commission on Water Resource Management, 57 p.

Camp Dresser and McKee, 1993a, Ground water modelling study: review of existing data, Ewa marina project: Report to Haseko (Ewa), Inc., Honolulu, Hawaii, September 1993, variously paged.

Camp Dresser and McKee, 1993b, Ground water modelling study: preliminary analysis of marina impacts, Ewa marina project: Report to Haseko (Ewa), Inc., Honolulu, Hawaii, December 1993.

Camp Dresser and McKee, 1994, Ground water modelling study: responses to CWRM comments on preliminary modelling, Ewa marina project: Report to Haseko (Ewa), Inc., Honolulu, Hawaii, May 1994, 68 p. + appendixes.

Cox, D.C., 1981, A century of water in Hawaii: *in* Groundwater in Hawai'i: A century of progress, Proceedings of the Artesian Water Centennial Symposium, November 29-

30, 1979, Fujimura, F.N., and Chang, W.B.C., eds., University of Hawaii Water Resources Research Center, 260 p.

Cox, D.C., and Lao, Chester, 1967, Development of deep monitoring stations in the Pearl Harbor ground water area on Oahu: University of Hawaii Water Resources Research Center Technical Report no. 4, 34 p.

Dale, R.H., 1968, Probable effects on ground water reservoirs by enlarging the harbor at Barbers Point, Oahu, Hawaii: U. S. Geological Survey Administrative Report to U.S. Corps of Engineers.

Fattah, Q.N., and Hoopes, J.A., 1985, Dispersion in anisotropic, homogeneous porous media: Hydraulic Division, American Society of Civil Engineering, v. 111, no. 5, p. 810-827.

Gelhar, L.W., and Axness, C.L., 1983, Three-dimensional stochastic analysis of macro-dispersion in aquifers: Water Resources Research, v. 19, no. 1, p. 161-180.

George A.L. Yuen and Associates, Inc., 1989, Ground Water resources and sustainable yield, Ewa plain caprock aquifer, Oahu, Hawaii: State of Hawaii, Department of Land and Natural Resources, Report, R-79, 50 p.+ appendixes.

Giambelluca, T.W., 1986, Land-use effects on the water balance of a tropical island: National Geographic Research, v. 2, no. 2, p. 125-151.

Hunt, C.D., Jr., in press, Geohydrology of the island of Oahu, Hawaii: U.S. Geological Survey Professional Paper 1412-B.

Ishizaki, Kenneth, Burbank, N.C., Jr., and Lau, L.S., 1967, Effects of soluble organics on flow through thin cracks of basaltic lava: University of Hawaii Water Resources Research Center Technical Report no. 16, 56 p.

Langenheim, V.A.M., and Clague, D.A., 1987, The Hawaiian-Emperor volcanic chain, part II, stratigraphic framework of volcanic rocks of the Hawaiian Islands, chap. 1 *of* Decker, R.W., Wright, T.L., and Stauffer, P.H., eds., Volcanism in Hawaii: U.S. Geological Survey Professional Paper 1350, v. 1, p. 55-84.

Lau, L.S., Dugan, G.L., and Hardy, W.R., 1986, Groundwater recharge with Honouliuli wastewater irrigation, 'Ewa plain, southern O'ahu, Hawai'i: University of Hawaii Water Resources Research Center Technical Memorandum Report no. 80, 45 p.

Lau, L.S., Hardy, W. R., Gee, H.K., Moravcik, P.S., and Dugan, G.L., 1989, Groundwater recharge with Honouliuli wastewater irrigation: 'Ewa plain, southern O'ahu, Hawai'i: University of Hawaii Water Resources Research Center Technical Report no. 182, 121 p.

Matsuoka, Iwao, Kunishige, V.E., and Lum, M.G., 1995, Water resources data Hawaii and other Pacific areas water year 1994, Volume 1: U.S. Geological Survey Water-Data Report HI-94-1, 435 p.

Miller, M.E., 1987, Hydrogeologic characteristics of central Oahu subsoil and saprolite: Implications for solute transport, M.S. thesis: University of Hawaii, 231 p.

Mink, J.F., 1980, State of the ground water resources of southern Oahu: Honolulu Board of Water Supply, 83 p.

Mink, J.F., and Lau, L.S., 1980, Hawaiian groundwater geology and hydrology, and early mathematical models: University of Hawaii Water Resources Research Center Technical Memorandum Report no. 62, 74 p.

Mink, J.F., Yuen, G.A.L., and Chang, J.Y.C., 1988, Review and re-evaluation of groundwater conditions in the Pearl Harbor groundwater control area, Oahu, Hawaii: State of Hawaii, Department of Land and Natural Resources, Report R-78, 95 p. + appendixes.

Nance, Tom, and McNulty, Tony, 1993, Summary of computer modeling of the Ewa limestone aquifer: Report to Haseko (Ewa), Inc., The Estate of James Campbell, Gentry Hawaii, Ltd., and Housing Finance and Development Corp.

Owenby, J.R. and Ezell, D.S., 1992, Monthly station normals of temperature, precipitation, and heating and cooling degree days, 1961-1990, Hawaii: NOAA Report, Climatography of the United States No. 81.

Resig, J.M., 1969, Paleontological investigations of deep borings on the Ewa plain, Oahu, Hawaii: University of Hawaii, Hawaii Institute of Geophysics Pub. HIG-69-2, 99 p. + appendixes.

Rumer, R.R., and Shiau, J.C., 1968, Salt water interface in a layered coastal aquifer: Water Resources Research, v. 4, no. 6, p. 1235-1247.

Silliman, S.E., Konikow, L.F., and Voss, C.I., 1987, Laboratory investigation of longitudinal dispersion in anisotropic porous media: Water Resources Research, v. 23, no. 11, p. 2145-2151.

Soroos, R.L., 1973, Determination of hydraulic conductivity of some Oahu aquifers with step-drawdown test data, M.S. thesis: University of Hawaii, 239 p.

Souza, W.R., and Voss, C.I., 1987, Analysis of an anisotropic coastal aquifer system using variable-density flow and solute transport simulation: Journal of Hydrology, v. 92, p. 17-41.

Stearns, H.T., 1939, Geologic map and guide of the island of Oahu, Hawaii: Hawaii Division of Hydrography, Bulletin 2, 75 p., map scale 1:62,500.

Stearns, H.T., 1946, Geology of the Hawaiian islands: Hawaii Division of Hydrography, Bulletin 8, 106 p.

Stearns, H.T., and Vaksvik, K.N., 1935, Geology and ground-water resources of the island of Oahu, Hawaii: Hawaii Division of Hydrography, Bulletin 1, 479 p.

Stearns, H.T., and Vaksvik, K.N., 1938, Records of the drilled wells on Oahu, Hawaii: Hawaii Division of Hydrography, Bulletin 4, 213 p.

Stearns, H.T., and Chamberlain, T.K., 1967, Deep cores of Oahu, Hawaii and their bearing on the geologic history of the central Pacific basin: Pacific Science, v. XXI, no. 2, p. 153-165.

Thrum, T.G., 1889, Artesian wells on Oahu, Hawaiian Almanac and Annual for 1889: Press Publishing Company Steam Print, Honolulu, Hawaii, p. 61-63.

Tom Nance Water Resource Engineering and Martin Markle and Associates Pty Ltd., 1991, Progress report on the effect of Haseko's proposed marina on the Ewa limestone aquifer: Report to Haseko (Hawaii), Inc., Honolulu, Hawaii.

Visher, F.N., and Mink, J.F., 1964, Ground-water resources in southern Oahu, Hawaii: U.S. Geological Survey Water-Supply Paper 1778, 133 p.

Voss, C.I., 1984, A finite-element simulation model for saturated- unsaturated fluid-density-dependent ground-water flow with energy transport or chemically-reactive single-species solute transport: U.S. Geological Survey Water-Resources Investigations Report 84- 4369.

Wentworth, C.K., 1938, Geology and ground water resources of the Palolo-Waialae District, Honolulu Board of Water Supply, Honolulu, Hawaii, 274 p.

Wentworth, C.K., 1951, Geology and ground-water resources of the Honolulu-Pearl Harbor area Oahu, Hawaii, Honolulu Board of Water Supply, Honolulu, Hawaii, 111 p.

Williams, J.A., 1976, Ground water leakage in the vicinity of the Barbers Point Barge Harbor, Oahu, Hawaii: Report to U. S. Corps of Engineers.